2022

Development of a synthetically modified fibronectin fragment as a building block for recyclable biomaterials

BOSTON UNIVERSITY

COLLEGE OF ENGINEERING

Thesis

DEVELOPMENT OF A SYNTHETICALLY MODIFIED FIBRONECTIN FRAGMENT AS A BUILDING BLOCK FOR RECYCLABLE BIOMATERIALS

by

WINNIE WANG

B.E., Stony Brook University, 2016

Submitted in partial fulfillment of the

requirements for the degree of

Master of Science

2022

Approved by

First Reader

Jeroen Eyckmans, Ph.D.
Research Assistant Professor of Biomedical Engineering

Second Reader

Wilson W. Wong, Ph.D.
Associate Professor of Biomedical Engineering

Third Reader

Mark W. Grinstaff, Ph.D.
William Fairfield Warren Distinguished Professor
Distinguished Professor of Translational Research
Professor of Biomedical Engineering
Professor of Chemistry
Professor of Materials Science and Engineering
Professor of Medicine

ACKNOWLEDGEMENTS

I would like to convey my sincere gratitude to my advisor, Dr. Jeroen Eyckmans, for his guidance and support during my time here. Thank you for your vision, encouragement, and generosity of your time and knowledge. I would also like to extend thanks to the members of my thesis committee: Dr. Wilson Wong and Dr. Mark Grinstaff, for their critical evaluation of my thesis. A huge thanks to Dr. Christopher Chen and the Tissue Microfabrication Lab, especially the wound healing team, for all of their contributions in helping me grow as a researcher and answering my many questions.

I wish to thank my family for their continuous support and the lessons they have imparted. I receive inspiration from my father, whose work ethic motivates me to keep striving for more. I am thankful to my partner, Alex, for his unconditional love and support on all of my adventures. Finally, I would like to thank my friends, old and new, for keeping me sane during a pandemic and for the cherished time spent together.

This work would not have been possible without all of you. I am endlessly grateful.

DEVELOPMENT OF A SYNTHETICALLY MODIFIED FIBRONECTIN FRAGMENT AS A BUILDING BLOCK FOR RECYCLABLE BIOMATERIALS

WINNIE WANG

ABSTRACT

Over the past few decades, the fields of tissue engineering and biomaterials have increasingly intersected to develop therapies designed for interaction with cells. While biomaterials with tunable mechanical and biochemical properties have been developed to direct cell behavior, the cell-material interface progressively changes as cells deposit new extracellular matrix (ECM) or degrade materials via hydrolytic or enzymatic digestion. One major challenge is that cells cannot actively remodel preexisting biomaterials into nascent tissue, thus signals that direct cell behaviors are gradually lost. Fibronectin (FN), a key player in the regulation of cellular processes and adsorption onto material surfaces, is readily remodeled during cell-mediated assembly of a fibrillar network during wound healing. Given new insights into the cell's ability to recycle preexisting FN, we explored the development of synthetically modified fibronectin, a class of synthetic biomaterials that can be delivered to wound environments and directly integrated into native ECM during remodeling. This thesis aims to (1) demonstrate proof-of-principle that synthetic materials can be integrated within newly formed ECM when conjugated to FN, (2) explore functional domains of FN and how they contribute to FN recycling, and (3) assess biofunctionality of synthetic materials after integration into newly formed ECM. We found that PEGylated FN can be recycled and deposited in a new provisional matrix by fibroblasts, although at a lower efficiency than full length FN labeled with AF488. To

better understand recycling and how specific functional domains within FN contribute to it, experiments were conducted with single domain FN fragments generated by proteolytic cleavage and with chimeric FN mimetics containing both cell binding and matrix-binding domains. While proteolytically cleaved fragments were degraded by cells, chimeric FN mimetics underwent limited recycling, suggesting that more than one domain may be necessary for recycling and that interactions with both ECM proteins and cells are required. Informed by these studies, new chimeric fibronectin fragments composed of ECM and cell binding domains were designed, cloned and inserted into a GST fusion vector to generate recombinant FN proteins with a higher efficiency of recycling. Finally, we demonstrated that fibroblasts recycle and integrate biotinylated FN in newly formed tissue, and biotinylated FN retains its bioactive sites for binding partners after undergoing recycling. Together, our studies suggest that coupling biomaterials to fibronectin is a promising strategy to integrate materials in native tissues.

TABLE OF CONTENTS

LIST OF FIGURES

LIST OF ABBREVIATIONS

AF	Alexa Fluor
DOC	Deoxycholate detergent
ECM	Extracellular Matrix
EDA	Fibronectin Extra Domain A
EDB	Fibronectin Extra Domain B
FN	Fibronectin
FN-AF488	Fibronectin labeled with Alexa Fluor 488
FN-PEG	PEGylated fibronectin
GST	Glutathione S-transferase
hpFN	Human plasma fibronectin
HRP	Horseradish peroxidase
IIICS	Fibronectin Alternatively Spliced Type III Connecting Segment
LAMP1	Lysosomal-associated membrane protein-1
MCF10A	Fibrocystic epithelial cell line
MW	Molecular Weight
NHDF	Normal human dermal neonatal fibroblast cells
PDMS	Polydimethylsiloxane
PEG	Polyethylene Glycol
PEGDA	Polyethylene Glycol Diacrylate
PH-SA-dex	Streptavidin conjugated dextran added post healing
PHSRN	Pro-His-Ser-Arg-Asn synergy peptide motif

RecFN	Recombinant fibronectin construct
RGD	Arg-Gly-Asp cell binding motif
RhFN	Rhodamine labeled fibronectin
SLLISWD	Multimerization peptide sequence
TBST	Tris buffered saline with 0.1% Tween
TF-SA-dex	Streptavidin conjugated dextran added during tissue formation
TGF-ß	Transforming Growth Factor Beta
VEGF	Vascular endothelial growth factor

1. INTRODUCTION

Background and Motivation for Research

Tissue engineering is a multidisciplinary field that applies engineering principles to provide solutions for regenerating or improving tissue structure and function. Introduced by Langer and Vacanti in 1993 [12], the general approach to tissue engineering consists of reparative cells to form a matrix, a scaffold to provide structural support, and a bioactive component which provides cues for desired cell behavior and tissue growth. Biomaterials, a rapidly evolving field regarding the engineering of synthetic or natural materials for use in clinical applications, naturally intersects with tissue engineering to provide substrates that can guide cellular processes in injured tissues and organs. Biomaterials with tunable mechanical and biochemical properties have been developed to achieve a more precise control of cellular responses including growth, migration, and differentiation [9]. However, upon introduction to a physiological environment, proteins are deposited onto biomaterials and become part of the biomaterials-cell interface that cells interact with and dynamically remodel. As cells deposit an ECM and/or degrade the material, the biomechanical and biochemical cues that direct cell behavior are gradually lost. Cells are also limited by their inability to remodel synthetic biomaterials and incorporate them into newly formed tissue, further reducing the bioactivity and functionality of biomaterials.

Fibronectin (FN) is a ubiquitous ECM glycoprotein that has an integral role in tissue repair and controlling cell response to biomaterials [18]. It acts as a communicator between the intracellular and extracellular environment of cells, and its adsorption

kinetics on the surface of biomaterials directly attributes to cell behaviors and their interaction with the biomaterial [9]. Thus, modulating how FN interacts with biomaterials can be key to retaining the synthetic control of materials. While cells are unable to remodel synthetic materials into nascent tissue, FN is readily remodeled during cell-mediated assembly of a fibrillar network during wound healing. In the context of tissue repair, FN regulates cell attachment and cell motility and becomes incorporated into a complex three-dimensional matrix made up of cellular FN deposited by fibroblasts, and preexisting FN that is recycled. It is well established that cells can recycle large molecules such as integrins and membrane receptors [4, 8, 26], but the extent to which ECM proteins such as FN can be recycled has not been well researched. The concept of recycling FN emerged in a study by Varadaraj, et al. in 2017 [32] via a TGF-β dependent trafficking mechanism and has been described by Sakar, et al. [22] through the towing, remodeling, and extension of existing FN into the provisional matrix of a wound. A recent study by Phillips, et al. found that overexpression of deubiquitinase USP10 reduces integrin degradation and results in an increase of both integrin and FN recycling after wounding [19]. Together, these studies suggest that FN is internalized by cells but not completely degraded; cells can reuse FN by secreting the internalized FN and incorporating them directly into a dynamic matrix, which provides a substrate for cells to migrate onto and continuously remodel. Given the cell's ability to recycle FN and a current challenge in integrating synthetic biomaterials into newly formed tissue, we hypothesize that **conjugation of synthetic materials to FN may serve as a method for integration of these materials into the microenvironment of newly formed tissue**

during wound healing, with the aim of retaining their signaling activity and biological functionality.

Thesis Overview and Research Aims

The overall goal of this thesis is to demonstrate proof of concept of integrative biomaterials: a class of synthetic biomaterials that can be integrated into the native ECM. To achieve this, our approach aims to exploit the recycling mechanism of fibronectin to integrate biomaterials into native ECM by engineering a synthetically modified fibronectin as a building block for recyclable biomaterials. By delivering a fibronectin-based synthetic material to wound environments, we can retain control of the synthetic materials after incorporation and create a new approach to studying cell-material interactions during tissue remodeling. A brief overview of the experimental aims is presented below:

- **Aim 1:** Demonstrate proof-of-principle that synthetic materials can be integrated within newly formed ECM when conjugated to fibronectin
- **Aim 2:** Explore functional domains of fibronectin and how they contribute to fibronectin recycling
- **Aim 3:** Assess biofunctionality of synthetic materials after integration into newly formed ECM

2. BIOMATERIALS BACKGROUND

At the interface between cells and biomaterials, ECM proteins adsorb and spontaneously assemble to form a provisional matrix that cells can recognize and dynamically remodel. The interactions of cells and this matrix comprises of two fundamental processes: assembly and degradation, which is regulated by material interfacial properties. Tailoring the mechanical and/or chemical properties of both interface and bulk parameters have been employed as techniques to drive changes in cellular behavior such as adhesion, proliferation, and differentiation. These parameters can provide biophysical cues such as hydrophilicity, surface topography, stiffness, and viscoelasticity, or biochemical cues such as growth factors and other bioactive molecules. However, these cues are progressively lost as cells continue to deposit ECM proteins or degrade the material. The main approach for tissue engineering with biomaterial constructs is to provide cells with a substrate such as a hydrogel or electrospun fibers that serves as a functionalized environment, which guides cell behavior and will be replaced by native ECM and cells over time. Although this method presents many advantages in traditional regenerative studies, cells are unable to remodel the scaffolding materials itself and cannot incorporate them into new tissues. By developing a synthetic biomaterial that cells can recycle and use as building blocks in producing new matrices, we anticipate that biological cues and reactive sites within the biomaterials will remain biologically active so that synthetic control of these materials can be retained.

Polyethylene glycol (PEG) and dextran are two extensively researched polymers that have been utilized in a range of tissue engineering applications due to their high

cytocompatibility and are well suited for use in hydrogels. PEG is a synthetic polymer that is hydrophilic, biochemically inert, and known to be resistant to protein adsorption [35]. It is widely used due to the versatility of its chemical structure; PEG can be linear or branched and can be functionalized with various end groups to covalently link biomolecules or build complex networks with tunable mechanical and chemical properties. Therefore, PEG has been used to simulate ECM matrices by modifying with bioactives such as antibodies, growth factor binding molecules, and cell adhesive peptide sequences like the RGD motif [16]. The most common method of PEG polymerization uses a photoinitiator and a UV light source to crosslink liquid PEGDA macromer solutions into a solid hydrogel. In a wound healing context, PEG has been used not only as hydrogels applied as wound dressing, but also as a protein modification on fibronectin to stabilize against proteolytic degradation [34]. Dextran is a biodegradable polysaccharide that has also been implicated in wound healing applications as modified dextran can be used to reduce inflammatory responses [2] and has been used as a coating to improve biocompatibility of other materials [25]. Dextran is easily modifiable with different functional groups due to its chemically reactive hydroxyl groups. Consequently, it can serve as a bioactive carrier for biomolecules as drug delivery systems or to reconstruct microenvironments with signaling cues for regenerative therapies. Both PEG and dextran have been fabricated into various structures such as tubules, spheres, fibers, and 3D networks [1, 5, 20, 27, 28], and the potential applications of both materials are yet to be fully explored.

3. FIBRONECTIN STRUCTURE AND FUNCTION

Modular Structure of Fibronectin

FN is a high molecular weight glycoprotein commonly found in the ECM and plays a central role in tissue repair and embryonic development. It interacts with cells and other matrix proteins to form a structural scaffold to regulate cell adhesion, cell migration, differentiation, proliferation, and other essential processes. FN exists as two forms: plasma and cellular FN. Plasma FN is secreted by hepatocytes and circulates with blood plasma throughout the body in a soluble form at a concentration of 300 µg/ml [17]. Cellular FN is produced by various cell types locally in a slightly less soluble compact

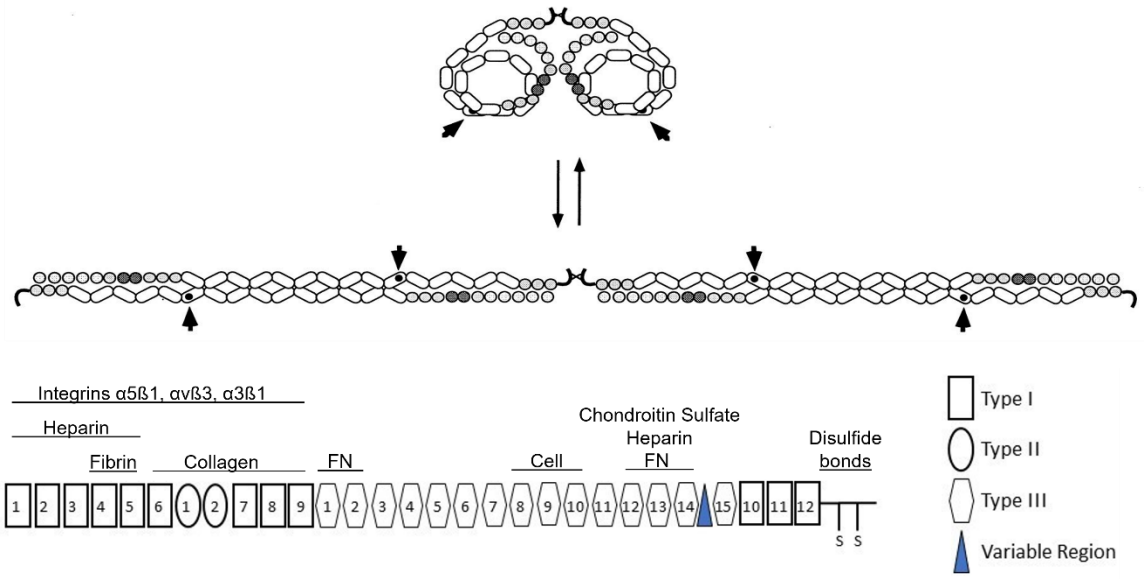

Figure 1: (A) Model of fibronectin in compact conformation dimerized via disulfide bonds at the C-terminus. Fibronectin undergoes cell-mediated assembly into an extended form that interacts with other FN fibrils, ECM molecules, and cells. Arrowheads indicate the RGD integrin binding site that becomes exposed after unfolding.

form and becomes irreversibly DOC detergent insoluble as its fibrils are assembled into a fibrillar matrix at the cell surface. FN undergoes this conformational change from inactive to active form via fibrillar assembly, a complex stepwise process mediated by

cells [14, 17]. In addition to interactions with cell surface receptors, its active form is interconnected with other FN fibrils and ECM proteins such as collagen, heparin, and chondroitin sulfate. These interactions are specific, and the binding regions are localized to defined modules of the FN protein (Figure 1).

FN consists of two similar subunits (~220-270 kDa) linked by a pair of disulfide bonds at its C-terminus (Figure 1). Each FN subunit is composed of repeated modules: twelve type I repeats, two type II repeats, 15 type III repeats, two alternatively spliced type III repeats that vary by isoform known as extra domain A (EDA) and extra domain B (EDB), and a non-homologous type III V region (known as IIICS in human FN) of variable length. Alternatively spliced EDA, EDB, and the variable region are found in some cellular FN isoforms but not in plasma FN. Type I modules are each made up of stacked ß-sheets protecting a hydrophobic core [14], while type II modules are comprised of two perpendicular anti-parallel ß-sheets connected with disulfide bonds. Type III modules have two anti-parallel ß-sheets linked by flexible loops. The modular structure and intermodular regions lend to the flexibility of the overall FN protein.

Matrix Assembly/Fibrillogenesis

FN remodeling is a dynamic process involving interactions between fibronectin, integrins, and cytoskeleton proteins. As mentioned, plasma and cellular FN are both expressed and secreted in a soluble globular form and require cells to unfold into an active form which assembles three-dimensional fibrillar matrix. The stages of matrix assembly can be broken down into initiation, unfolding, and fibrillogenesis. Initiation occurs via binding of cell surface receptors to FN (Figure 2A), activating integrin

signaling to regulate adhesion complex formations. Integrin binding induces reorganization of actin and myosin which generates contractile forces (Figure 2B), aiding in the unfolding of tethered FN molecules to expose cryptic binding sites hidden within the compact structure. The extended structure allows FN-FN intermolecular interactions to occur (Figure 2C), forming a continuous extension of FN fibrils that overlap and crosslink into stable multimers. During early stages of fibrillogenesis, fibrils are thin and short, extending only between adjacent cells or between cells and substrate. As fibrils

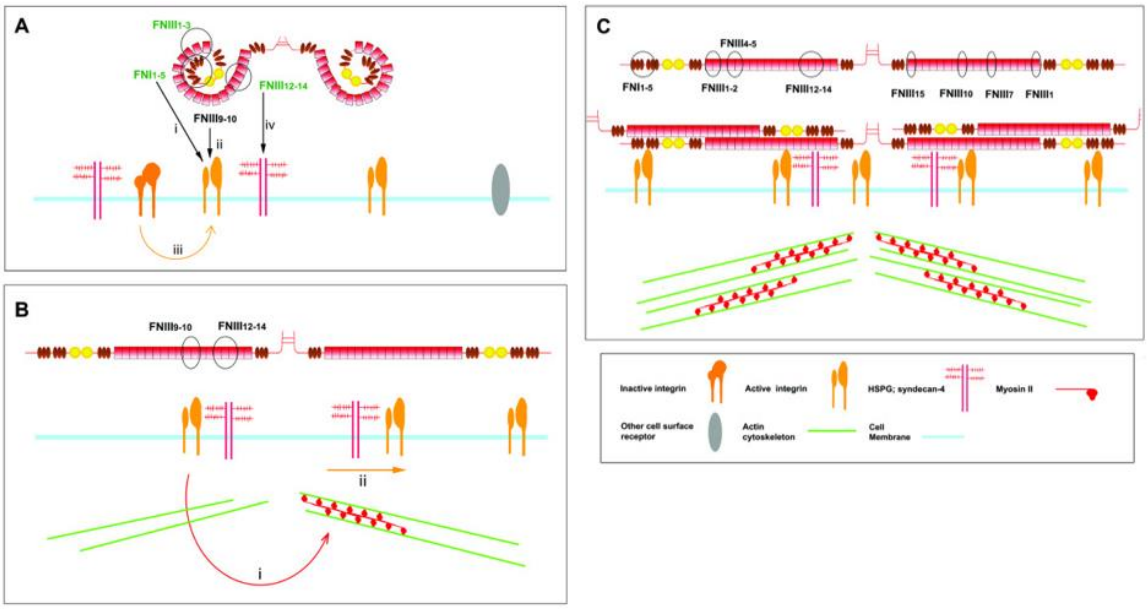

Figure 2: Model of stages of FN. (A) Initiation involving binding of FN to cell surface receptors. (B) Unfolding of tethered FN molecules; outside-in and inside-out integrin activation induces formations of focal adhesions and cytoskeletal changes that aid in unfolding. (C) Exposure of cryptic binding sites that allow for FN-FN interactions, elongation of fibrils, and lateral thickening into complex fibrillar matrices. Fibrillar matrices are continuously remodeled and can detach, stretch, retract, and anneal [30].

grow in length and diameter, they are irreversibly assembled into a stable DOC-insoluble matrix, a process that has not yet been elucidated. These stepwise conformational changes convert FN into an active form that can be continuously reorganized by cells

based on their needs, in addition to serving as a substrate for deposition of other ECM proteins and a reservoir for growth factors.

Based on current models, the compact form is maintained by electrostatic interactions between I_{1-5}, III_{1-2}, III_{2-3}, and III_{12-14} [6]. The 70 kDa domain is involved in initial binding to the cell surface; the exact cell surface receptors have not yet been elucidated but various integrins have been found to interact with repeats I_{1-5}. Recombinant FN lacking the 70 kDa region is unable to undergo fibrillogenesis, and excess 70 kDa fragments block matrix assembly [24]. The 70 kDa domain can identify sites of assembly due to its recognition of multiple binding partners, making it essential for the assembly process and controlling alignment of FN dimers based on which partners are available. The RGD sequence and synergy site within III_{9-10} binds to integrin α5ß1, an essential step to assembling complex fibrillar networks [6, 29]. In most instances, FN assembly is initiated by integrins that recognize the RGD and synergy sequences. Surprisingly, the specific location of the cell-binding site within FN is not critical; recombinant FN that replaced repeats III_{4-5} with III_{9-10} had no effect on assembly [23]. Chimeric FN constructs that insert an RGDS loop into III_8 coupled directly to a small heparin binding domain at III_{1H} were found to support cell adhesion, proliferation, and ECM assembly on substrates coated with them [21]. Therefore, the integrin-binding site does not need to be centrally located for initiation and propagation of FN fibril formation. While groups have conducted critical research on the functional domains of fibronectin by generating recombinant fibronectin to determine their importance and elucidate mechanisms in matrix assembly, the domains involved in recycling have not yet been investigated.

Fibronectin Domains and their Known Functions

FN is a ligand for a large number of integrins and ECM proteins such as fibrin, collagen, heparin, and more. Extensive analyses done by recombinant protein or proteolytic fragmentation have elucidated functionally important domains and cell recognition sequences. Proteolytic cleavage of fibronectin by thrombin, trypsin, cathepsin D, thermolysin, plasmin, and chymotrypsin results in fragmentation in highly specific sites, yielding a 70 kDa, 120 kDa, and 40 kDa fragment from the amino- to carboxyl-terminus (Figure 3) [6]. The 70 kDa fragment at the N-terminus, consisting of consists of repeats I_{1-6}, II_{1-2}, and I_{7-9}, is known as the assembly domain and is required for interactions with binding sites across FN, heparin, fibrin, and integrins α5ß1, αvß3, and α3ß1. It can be further digested into 30 kDa (I_{1-6}) and 45 kDa (II_{1-2}-I_{7-9}) fragments. The 120 kDa fragment, or the central binding domain, consists of repeats III_{1-12} and most notably interacts with integrin α5ß1 via the RGD sequence in III_{10} required for initiation of matrix assembly [24]. The PHSRN sequence of the synergy site located in III_9 modulates accessibility of the RGD motif to assist in cell binding but is not required for matrix assembly [30]. III_{9-10} also recognizes integrins αvß3, αvß1, αvß6, α8ß1 and αIIbß3. Cryptic binding sites for FN-FN association are exposed during FN unfolding to advance fibrillogenesis. These domains include repeats III_{1-2}, which recognizes repeats I_{1-5} and III_{12-13}; and $III_{7,}$ III_{10}, and III_{15}, which all can bind III_1. Multimerization activity is localized to the sequence SLLISWD in repeat III_{10}, which becomes exposed during unfolding [7].

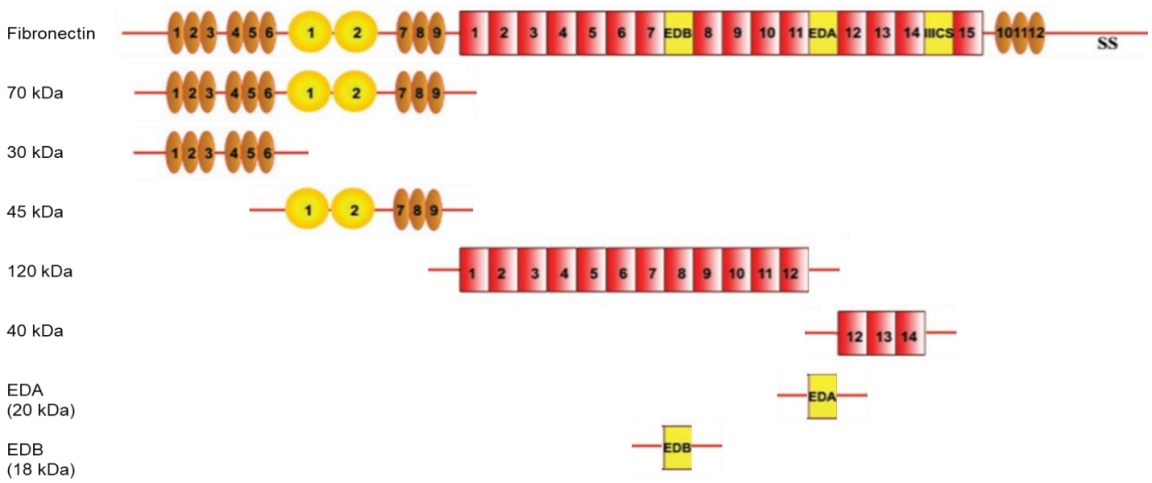

Figure 3: Fragments of varying molecular weights attained from proteolytic digestion of human plasma fibronectin. Figure adapted from [30].

Collagen, another important ECM protein, has a binding partner with FN at repeats II_{1-2}-II_{7-9}. Heparin and chondroitin sulfate recognize the 40 kDa fragment, which is made up of repeats III_{12-14}. Heparin binding activity has also been found in repeat III_1, a cryptic site that is exposed during matrix assembly [11]. FN is also known to sequester growth factors such as TGF-ß, VEGF, and BMP1 that regulate its continuous remodeling by cells [30]. Repeat III_{12-14} presents a growth factor binding site that works synergistically with integrin signaling on the neighboring cell binding region at repeats III_{8-10} [15]. Finally, the carboxyl terminal cysteines are necessary for dimerization of the FN subunits via a pair of disulfide bonds, as monomeric FN are not capable of fibrillogenesis.

During early wound healing events, plasma FN is incorporated into fibrin clots for stabilization and regulate platelet and cell adhesion, spreading, and aggregation. Fibrin interacts with repeats I_{4-5} and I_{10-12} and is covalently crosslinked to FN as a result of the blood coagulation cascade involving activated Factor XIIIa [3]. Cellular FN isoforms are more active in late repair events, with cells synthesizing a dense network around

themselves and assembling a three-dimensional fibrillar matrix to serve as structural framework and allow migration of cells to repopulate the wound. Alternatively spliced isoforms containing EDA and EDB domains are upregulated in granulation tissue during neovascularization; EDA and TGF-ß are required for myoblast differentiation and are associated with changes in the mechanical properties of the wound. EDA and EDB are present in embryonic vessels but not in adult vessels, only reappearing during pathological angiogenesis or tissue regeneration processes. Mice with both EDA and EDB knockouts did not survive to birth, having improperly formed vessels and endothelial cell sheets. The effects of single domain knockouts are less obvious, indicating there may be some redundant function but at least one is necessary for normal vessel development and wound healing [33].

4. FIBRONECTIN RECYCLING

Mechanism of Fibronectin Recycling

Cells are known to be able to recycle large molecules such as integrins and receptors via endocytosis, but pathways for recycling ECM proteins are yet to be described or elucidated. Emerging studies indicate that FN can be recycled into a nascent matrix, especially during embryogenesis and wound healing events. Varadaraj, et al. were the first to describe FN recycling in 2017 via a TGF-ß dependent mechanism which found internalization but not degradation of FN from the cell surface, and the direct reincorporation of internalized FN into fibrils [32]. Rhodamine labeled FN (RhFN) was added to MCF10A cells and incubated for 30 minutes to allow uptake, washed with acid to strip off surface proteins, and fixed for immunostaining. It was observed that the bulk of internalized RhFN was not localized to lysosomal protein LAMP1 within 6 hours of TGF-ß treatment, which is well within the period for non-transcriptionally regulated fibrillogenesis (Figure 4C). To assess if internalized FN directly contributed to the DOC-insoluble matrix, biotinylated FN was incubated with cells, washed, and allowed to recover for 1 hour in media with or without TGF-ß. Lysates were DOC fractionated into soluble and insoluble (pellet) fractions and immunoblotted with streptavidin-conjugated IR dye to detect and quantify the recycled biotin-FN (Figure 4E), showing that TGF-ß increased the insoluble fraction of biotin-FN. This was visualized with RhFN (Figure 4G) to confirm that the recycled FN came from the internalized pool.

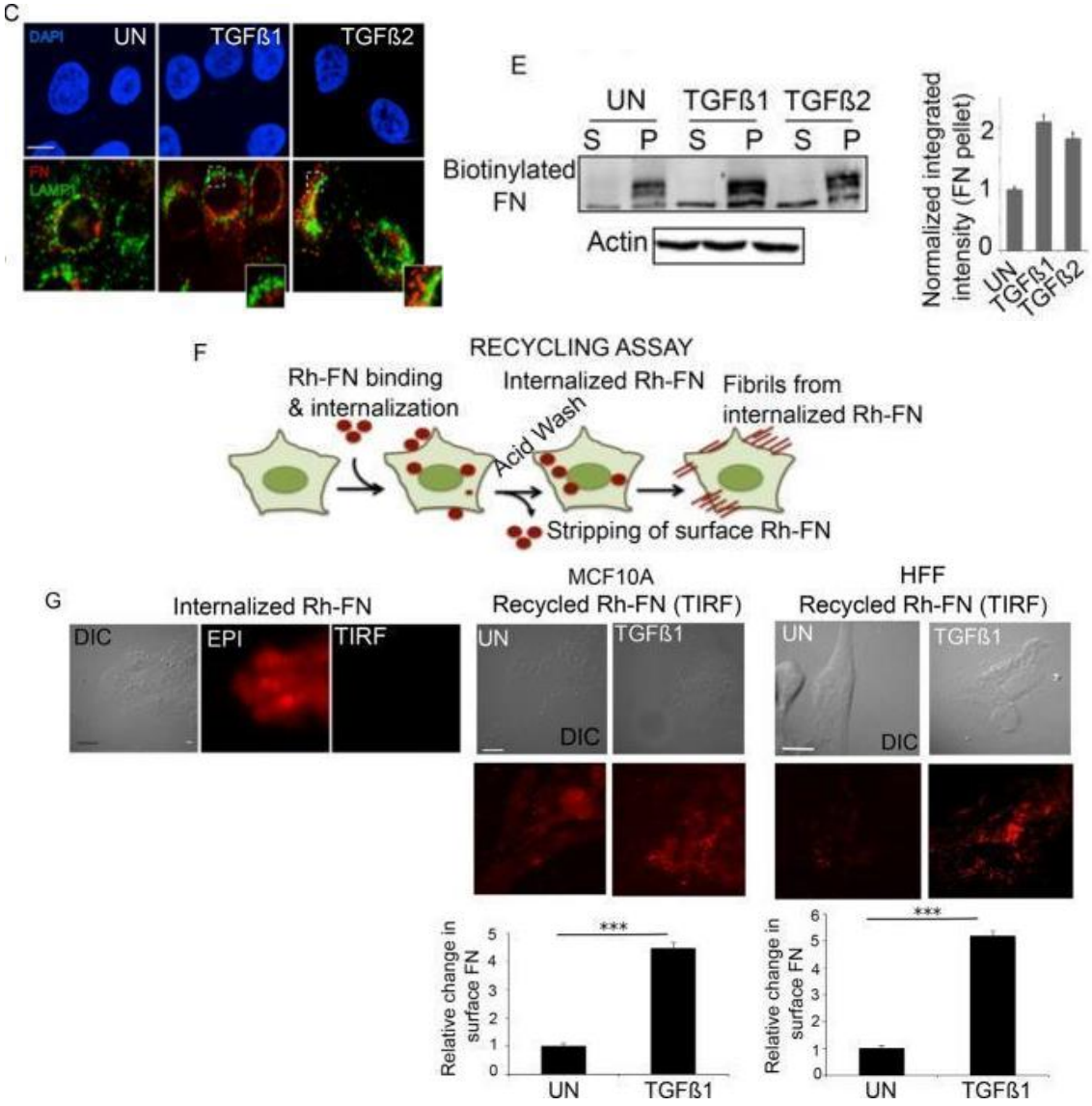

Figure 4: TGF-ß increases internalization and recycled FN is directly incorporated into the DOC-insoluble matrix. (C) MCF10A cells untreated, treated with TGF-ß1, or TGF-ß2 immunostained with anti-LAMP1 and anti-FN. (E) Insoluble biotin-FN from DOC-fractionation and detected with streptavidin-IR dye. (F) Recycling assay schematic with RhFN used for G. (G) Internalized RhFN confirmed with Epi and TIRF illumination shows increased reappearance on cell surfaces in cells treated with TGF-ß1. Figure adapted from [32].

Deubiquitinase gene USP10, which is upregulated in human corneal myofibroblasts in pathological conditions, has been shown to prevent degradation of fibroblasts by increasing integrins α5ß1 and αv recycling to the cell surface via decreased

ubiquitination, subsequently promoting FN recycling as well [19]. In a similar recycling assay, biotinylated FN was exogenously added to transfected cells, and the recycled biotinylated FN was found to make up a third of total FN.

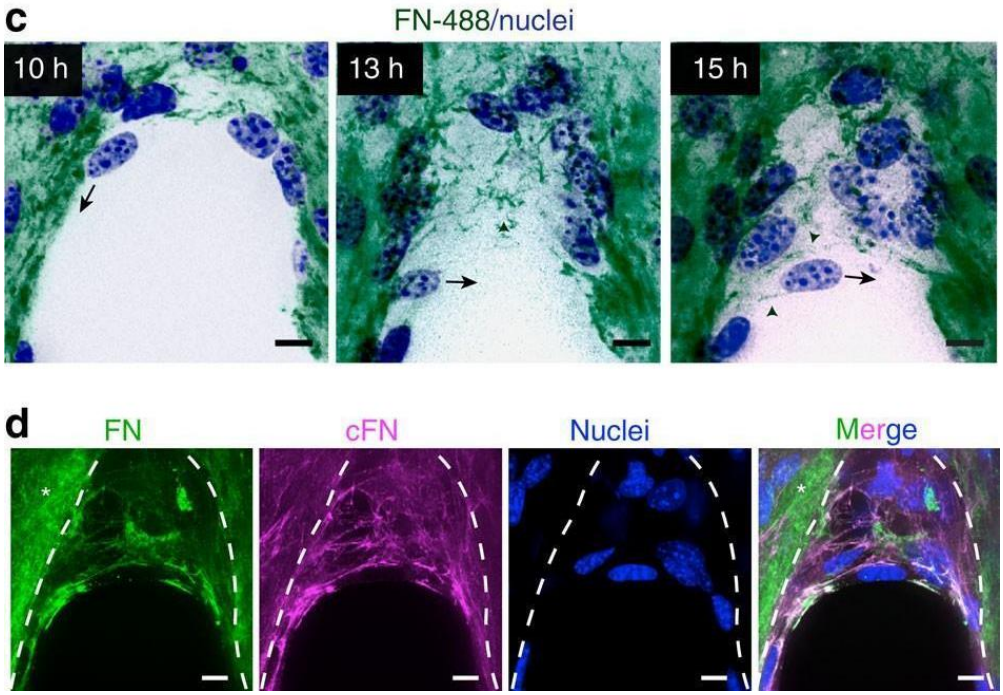

Figure 5: (C) Time lapse of fluorescently labeled FN at wound edge and migration direction of cells during closure. (D) Exogenously added FN is remodeled into the provisional matrix along with cellular FN deposited during wound closure. Immunostaining of total fibronectin (green), cellular fibronectin (magenta), and nuclei (blue) [22].

The dynamics of FN matrix assembly can be also tracked using fluorescence microscopy to reveal motility, extension, and multimerization of fibers as they are deposited and remodeled. In a 3D wound healing assay, Selman, Eyckmans, and colleagues administered fluorescently tagged plasma fibronectin to injured microtissues [22]. They observed that fibronectin fibers composed of exogenous fluorescently labeled fibronectin is recruited by cells within a collagenous microtissue, deposited into a gap area after injury, and continuously remodeled by fibroblasts into the provisional matrix during gap

closure at later time points to colocalize with newly deposited cellular fibronectin (Figure 5).

Taken together, these studies suggest cells' ability to internalize and reuse soluble FN via mechanisms that are not limited to TGF-ß dependent trafficking mechanisms. Though previous studies emphasize internalization as part of the recycling pathway, we define recycling as the incorporation of any preexisting fibronectin fibrils into the assembly of a new matrix.

Wound Healing Platform to Assess Recycling

The wound healing testbed introduced by Sakar, et al. is a 3D culture system that recapitulates a wound healing environment in stromal microtissues [22]. The microtissues are injured and can be monitored as the wound closes to examine the response of the tissue to damage. Similar to the devices described in Sakar, et al., rectangular wells with four capped standing pillars are fabricated with PDMS. After seeding of a fibroblast/collagen type I suspension, cells compact the polymerized collagen matrix around the pillars to generate 3D microtissue. Full thickness wounds are generated using a laser pulse after overnight incubation in cell growth medium, and the ensuing wound closure can be monitored with time lapse microscopy. This system allows for the complexity of a wound environment to remain controlled while simulating the ECM in a three-dimensional space, allowing cells to coordinate matrix assembly that is not limited to 2D substrates. More importantly, it provides a window to observing fibronectin recycling during assembly of the provisional matrix. By introducing exogenous fibronectin to the microtissues during tissue formation, we can assess how fibronectin

fibers are recruited by cells during wound healing and if they directly contribute to the provisional matrix after wound healing.

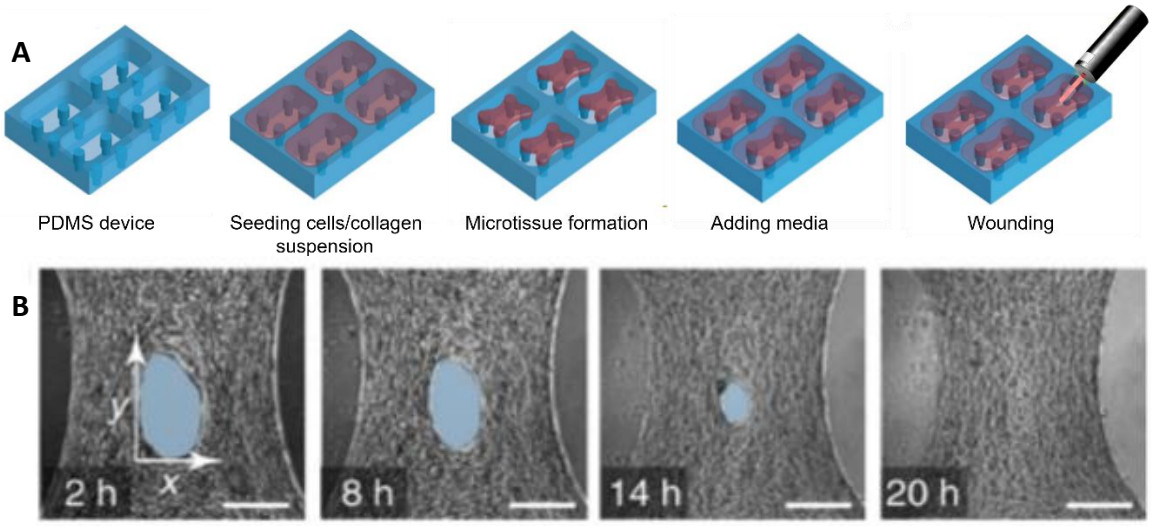

Figure 6: (A) Workflow of wound healing device seeding and injury. (B) 2h, 8h, 14h, and 20h time points after injury showing closure of wounded gap area [22].

5. METHODS

Wound healing device fabrication

Single devices are fabricated in 96-well plates using stamps for individual wells. A CAD model of an inverse micropillar mold was printed via two-photon polymerization using a Nanoscribe 3D printer. The mold was treated in a plasma asher for 30 seconds, then silanized using vapor-deposition for 6 hours. A copy of the mold was made with Polydimethylsiloxane (PDMS, Dow-Corning Sylgard 184) mixed at a 1:10 ratio and cured overnight at 60° C. Multiple PDMS molds were used to cast a hard resin mold (Smooth-On, Task 3™). PDMS is poured into the resin mold, degassed in a vacuum chamber to remove air bubbles, and were baked overnight at 60°C, yielding a soft working mold. The working mold is plasma-treated and silanized, then filled with PDMS and baked at 60° C to yield stamps with individual micropillar devices. The stamps are

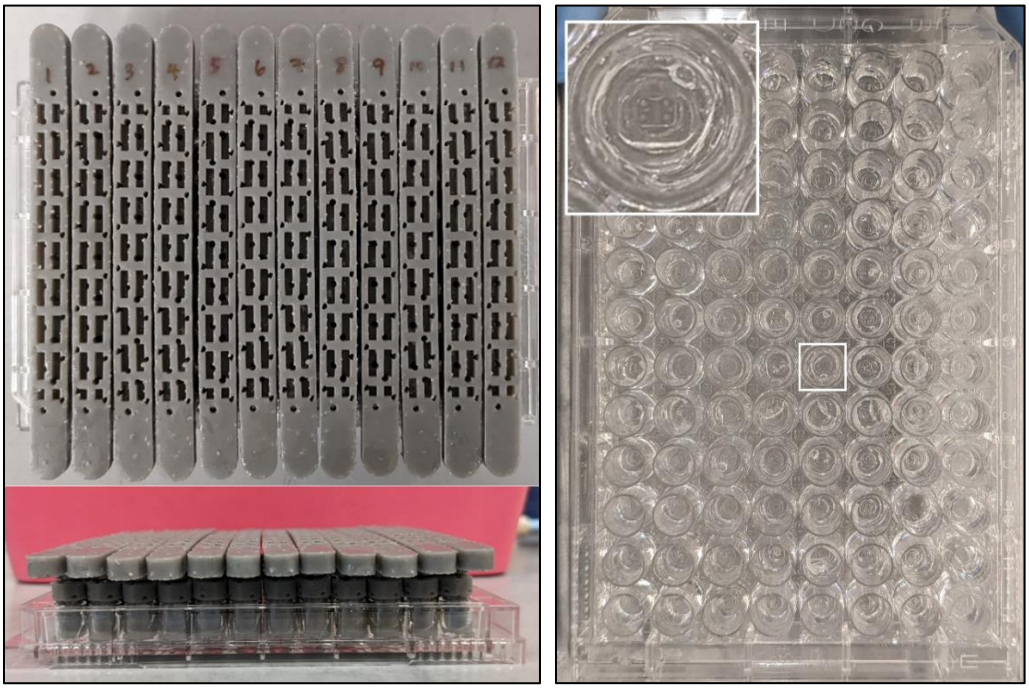

Figure 7: 3D printed racks (left) containing PDMS stamps used to fabricate devices in a 96-well plate (right).

assembled into 3D-printed racks which positions an inverted stamp into each well. The stamps and racks were plasma-treated, then silanized for at least 6 hours. ~15 uL of PDMS is added onto each stamp and 70–90 uL of PDMS is added into each of the wells. After degassing, the racks are inserted into the 96 well plate and baked at 60°C overnight. 70% ethanol is used to aid in removal of the racks, leaving an individual device in each of the 96 wells. Devices are cleaned using sonication with 70% ethanol for 30 minutes, followed by ultraviolet sterilization for 15 minutes, and overnight incubation with sterile H_2O. Prior to microtissue seeding, each device is treated with 0.02% pluronics-F127 (Sigma) for 10 minutes at 37°C and washed twice with sterilized H_2O.

Cell Culture

Primary neonatal human dermal fibroblasts (Lonza) were cultured in FGM™-2 Fibroblast Growth Medium (Lonza) and passaged with 0.05% Trypsin-EDTA at ~90% confluence. Cells under passage 10 were used for these experiments.

Fibronectin Reagents

Human plasma FN (Life Technologies) was PEGylated with 5kDa heterobiofunctional linear PEG with a fluorescein dye and carboxylic acid group (Creative PEGWorks) at a 9:1 molar ratio via NHS/EDC chemistry. Briefly, a PEG solution was prepared at 1 mg/mL in activation buffer (0.1 M MES, 0.5 M NaCl, pH 6) and reacted with 2mM EDC and 5mM NHS for 15 minutes at room temperature. 20 mM of 2-mercaptoethanol was added to quench the reaction. Immediately before mixing with FN, the pH is increased to 7.2-7.5. PEG was added into the FN solution at a 9:1 molar ratio and reacted for 2 hours at room temperature, followed by 10 mM of hydroxylamine to promote hydrolysis of

NHS esters on PEG to regenerate unreacted carboxyl groups. Excess reagents were dialyzed overnight with PBS using Slide-A-Lyzer™ cassettes (Thermo Scientific). The concentration of FN-PEG was determined using a NanoDrop™ spectrophotometer.

To visualize FN matrices within microtissues, proteolytic FN fragments, EDA, and EDB were labeled with Alexa Fluor dyes (Life Technologies). FN proteolytic fragments of molecular weight 120 kDa, 40 kDa, 30 kDa, 45 kDa, and 70 kDa (Sigma) and recombinant human EDA (Abcam, ab157273) and EDB proteins (Abcam, ab209886) were dissolved in sterile H_2O at 1 mg/mL. AF NHS esters were reconstituted in dimethyl sulfoxide, added to FN at a 9:1 (AF:FN) molar ratio, and reacted at room temperature for 2 hours. The protocol was repeated for full length hpFN (Life Technologies). Excess reagents were dialyzed overnight with phosphate buffered saline using Slide-A-Lyzer™ cassettes (Thermo Scientific). The concentrations of all FN reagents were individually determined using a NanoDrop™ spectrophotometer.

Biotin-FN was generated using EZ-Link™ NHS-Biotin (MW: 341.38 g/mol, Thermo Fisher) at a 20:1 molar ratio.

Chimeric FN mimetics GST/III1H,8–10, GST/III1H,8,10, and GST/III1H,8^{RGD} (Figure 8A) were obtained from Dr. Denise Hocking (University of Rochester) and were generated as described in [10]. These proteins were labeled with Alexa Fluor NHS esters using the protocol described above. Briefly, human fibronectin cDNA was PCR-amplified to produce the desired sequences and cloned into pGEX-2T to obtain the GST-tag, then transfected into DH5α bacteria. Proteins were isolated on glutathione agarose, then heparin-Sepharose beads.

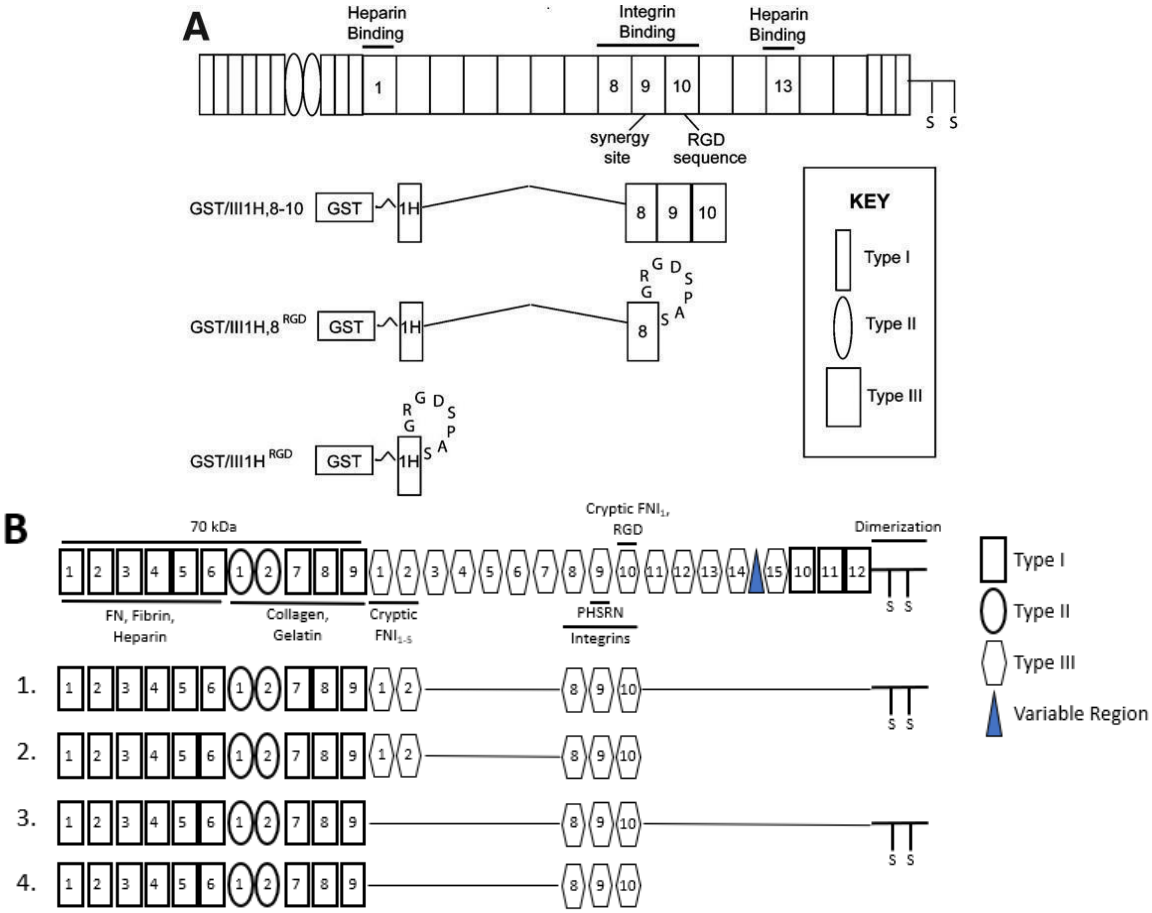

Figure 8: (A) Schematic representation of chimeric FN mimetics adapted from [21]. (B) Schematic of recombinant FN proteins designed for increased recycling efficiency (RecFN1-4).

Four recombinant protein constructs designed to increase efficiency of recycling are shown in Figure 8B. Human plasma fibronectin (Addgene plasmid #120401) was used as a template to produce each of the fragments, which are cloned into a GST fusion vector (Addgene plasmid #22227) via Gibson assembly. The 70 kDa domain and III_{1-2} fragment in RecFN1-2 was amplified with PCR using the forward primer 5'-ccaaaatcggatctggttccgcgtggatccatgcttaggggtccgggg-3' and reverse primer 5'-ccctcactctagagtcgcggccgcatcgatggtaccatcaggcgctgt-3'; the III_{8-10} fragment for RecFN1-2 was amplified using the forward primer 5'-

ctgtctacttcacaaacaacagcgcctgatgctgttcctcctcccactg-3’ and reverse primer 5’-ctctagagtcgcggccgcatcgatggtaccgtcaatttctgttcggtaattaatggaaat-3’. For RecFN3-4, the same forward primer is used to amplify the N-terminus fragment (5’-ccaaaatcggatctggttccgcgtggatccatgcttaggggtccgggg-3’) with the following reverse primer: 5’- ctctagagtcgcggccgcatcgatggtaccgacgggatcacacttccacc-3’; the $III_{8\text{-}10}$ fragment for RecFN3-4 was amplified using the forward primer 5’-ggtcggggcaggtggaagtgtgatcccgtcgctgttcctcctcccactg-3’ and the same reverse primer (5’-ctctagagtcgcggccgcatcgatggtaccgtcaatttctgttcggtaattaatggaaat-3’). The C-terminus fragment containing disulfide bonds in RecFN1 and RecFN3 was produced with forward primer 5’- atttccattaattaccgaacagaaattgacgggggtgaacccactcc-3’ and reverse primer 5’-agtcgcggccgcatcgatggtaccactagtttactctcgggaatcttctctgtc-3’. KpnI sites are underlined. All plasmids were assembled sequentially; the GST backbone vector is double digested using BamHI and KpnI before inserting the N terminus fragments, then reopened with KpnI and calf-intestinal phosphatase, followed by insertion of the central binding domain. For RecFN1 and RecFN3, the digestion step is repeated for insertion of the C-terminus fragments. Gibson assembly products are transfected into NEB® 10-beta competent *E. coli* cells and plasmids are isolated with the Qiagen Spin Miniprep Kit (QIAGEN). A diagnostic restriction digest is run by incubating each of the four plasmids with XmaI and KpnI, which have restriction sites that flank the full insert. The digested plasmids are run on a 1% agarose gel to determine the relative sizes of resulting fragments and imaged through a UV light box.

Wound healing experiments to assess fibronectin recycling

200 µL of collagen solution prepared with NaHCO3, HEPES buffer, Medium 199, sterilized H_2O, NaOH, and rat tail type I collagen (Corning) at a final concentration of 2.2 mg/mL is mixed with 1.4 million NHDF cells. 1.1 µL of the cell-collagen solution is pipetted into the center of each well while the device remains cooled on the ice block to prevent polymerization. The device is firmly struck onto a benchtop to uniformly disperse the solution and cover the surface area of the well. The device is incubated at 25°C for 10 minutes while inverted at room temperature to allow cell dispersion to the surface of the collagen followed by inverted incubation at 37°C for 15 minutes. A drop of phosphate buffered saline is added to the lid above each well to reduce drying of tissues during polymerization. For the FN-PEG dosage experiments, 100 uL of FGM^{TM}-2 with 50 nM, 150 nM, or 250 nM of FN-PEG is added to the devices. Experiments for aim 2 use FN fragments and chimeric FN mimetics which are spiked into the media at 50 nM. Full length fibronectin labeled with AF488 dye (50 nM) is used in positive control tissues.

Biotinylated-FN experiments for aim 3

Microtissues are formed using the same method described above. Biotin-FN was exogenously added during tissue formation at 50 nM. To detect if biotin sites are still functionally active and available, live tissues were exposed to AF488 streptavidin (1:100, gift from John Ngo lab) for 1h after the tissues were healed, or 24 hours after injury. In an effort to generate fibrillar structures with exogenous materials, streptavidin conjugated dextran (SA-dex) (FinaBio, 250 kDa) was added to tissues with biotin-FN at two time

points: 1 hour after seeding during tissue formation, and 24 hours after injury.

Wounding and Gap Closure Analysis

Full thickness wounds are inflicted at the center of each microtissue using a 1 mJ laser pulse 1068 nm. Time lapse microscopy was set up to acquire phase contrast images every 30 minutes over a 24-hour period. Images are analyzed with ImageJ to measure the empty space within the wound and calculate gap closure rate. A one-way ANOVA was performed on the means and followed by a Tukey *post-hoc* test for normal data. For nonparametric data, a Kruskal-Wallis test was performed, followed by a Dunn test with Bonferroni correction. Significance values are indicated as *$P \leq 0.05$, **$P \leq 0.01$, and ***$P \leq 0.0001$.

Immunohistochemistry

Microtissues were fixed with 4% paraformaldehyde and blocked with 10% goat serum for 1 hour at room temperature. Total fibronectin in the microtissues is detected with polyclonal Rb anti-fibronectin or monoclonal Ms anti-fibronectin (Abcam, 1:100) and was incubated for 1 hour at room temperature. EDA and EDB were detected with polyclonal Rb anti-DYKDDDDK tag (Cell Signaling, 1:100) and Ms monoclonal 6x-His antibody (ThermoFisher, 1:100), respectively. All primaries were followed by overnight incubation with DAPI (Invitrogen, 1:1000) and goat anti-rabbit/anti-mouse AF568 conjugated antibodies (Abcam, 1:1000) at 4°C. For the PEG dosage experiments, Ms anti-FITC (1:100, gift from John Ngo lab) was used against FN-PEG to detect the FITC group, followed by incubation with goat anti-mouse AF488. Anti-dextran with a FITC conjugate (StemCell Technologies, 1:100) was used to detect SA-dex.

Microscopy

To visualize the ECM, images labeled by immunostaining were captured on the Leica SP8 confocal microscope using a Leica 25X water objective on the Leica LAS X imaging software platform. Composite images were manually Z-stacked in ImageJ, and brightness and contrast were adjusted for fluorescence images in ImageJ.

Western Blot Analysis

PEGylation of FN was confirmed by immunoblotting using standard procedure. 1 µg of hpFN, FN-AF488, and FN-PEG was electrophoresed on a 3-8% gradient Tris-Acetate gel, transferred to a polyvinylidene difluoride (PVDF) membrane for 16 hours at 30 V in a cold room, and blocked with 5% nonfat milk in TBST for 1 hour at room temperature with agitation. The membrane was probed with polyclonal anti-FN (Abcam, 1:5000) overnight at 4°C with agitation, washed thrice with TBST at 15 minutes each, then incubated with anti-rabbit HRP (Cell Signaling, 1:50000) for 1 hour. The membrane is washed three times with TBST at 15 minutes each, then incubated with SuperSignal West Pico chemiluminescent reagents (Pierce) and imaged with the iBright FL1500 imaging system (Thermo Fisher) to detect positive bands. The membrane is stripped using a mild stripping buffer (15 g glycine, 1 g SDS, 10 mL Tween 20, total volume 1 L, pH 2.2). Immunoblotting steps are repeated with anti-FITC primary antibody (gift from John Ngo lab, 1:5000) to confirm PEGylation of the FN.

6. RESULTS

Aim 1: Demonstrate proof-of-principle that synthetic materials can be integrated within newly formed ECM when conjugated to FN

PEGylation of lysine residues on FN

Lysine residues of FN were PEGylated by heterobifunctional NHS-PEG-FITC reagents of molecular weight 5kDa (Figure 9A). The immunoblotting results using fibronectin and FITC detection are shown in Figure 9B. The increase in molecular weight of the FN-PEG is unclear, possibly due to interactions of PEG with the gel that cause smearing or nonspecific binding with the antibody. Anti-PEG antibodies can have a low affinity to its target and therefore have difficulties in immunoblotting applications. Therefore, anti-FITC was used to confirm the presence of FITC, and therefore PEG groups, on FN-PEG.

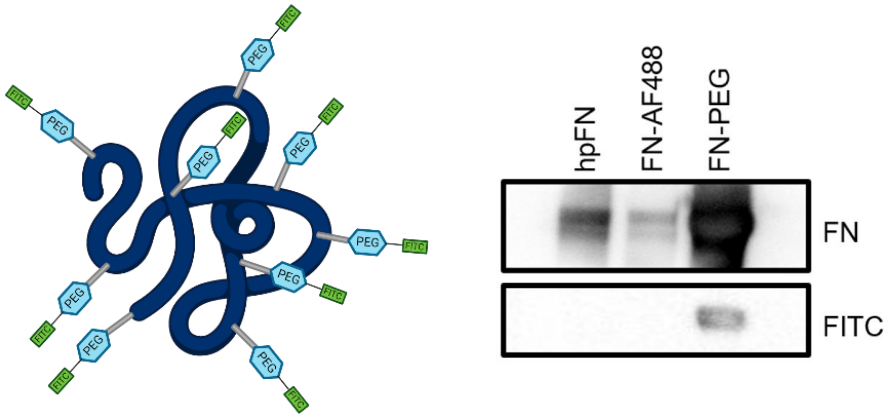

Figure 9: (A) Representation of FN-PEG: fibronectin conjugated with 5kDa PEG-FITC groups at a 9:1 (PEG:FN) molar ratio. (B) Western blotting of hpFN (Lane 1), fibronectin labeled with AF488 (Lane 2) and PEGylated fibronectin (Lane 3) showed that only FN-PEG is positive for FITC, which is conjugated to PEG. 1 µg of protein per lane was electrophoresed on a 3-8% Tris-Acetate gel and transferred to a PVDF membrane. The blot was blocked with 5% nonfat milk in TBST and incubated with polyclonal anti-FN (primary) and goat anti-rabbit HRP (secondary) before staining with the SuperSignal™ West Pico PLUS Chemiluminescent Substrate kit. The membrane was stripped and reblocked, incubated with anti-FITC (primary) and goat anti-mouse HRP (secondary), and stained with the same kit. Negative control is hpFN and FN-AF488 for FITC.

Synthetic materials can be recycled when conjugated with fibronectin

We demonstrate that PEG, when conjugated with fibronectin, is integrated into the provisional matrix of a wounded microtissue during tissue healing. Wound closure is contributed to by contraction of existing collagen matrix as well as assembly of new matrix within the gap, which serves as a substrate for cells to migrate into to remodel the matrix. PEGylated fibronectin that was exogenously added during tissue formation before tissue injury is found in this newly deposited tissue that has formed during healing (Figure 10). In addition to the provisional matrix being positive for FITC, the fluorescent signals appear to be assembled in fibrillar structures, as highlighted in insets in Figure 10. The total fibronectin matrices of the tissues with exogenous PEGylated fibronectin retain normal architecture. Gap closure rates, which measure the slope of the decrease in wound gap area, were measured using time lapse microscopy and ImageJ analysis to determine effects of FN-PEG on wound healing. Addition of FN-PEG also does not appear to inhibit wound closure; the FN-PEG dosage study found no significant difference between gap closure rates in tissues with added FN-AF488 (control) at 50 nM and tissues with FN-PEG (50 nM). However, there were significant differences in gap closure rates between the control group and FN-PEG added at 150 nM and 250 nM in which the latter groups had a lower slope, indicating faster closure (Figure 11). Unpublished data shows that increasing concentration of fibronectin slows down wound healing, contradicting the data shown for FN-PEG. These findings suggest that synthetic materials such as PEG can be integrated into the provisional matrix without impacting native ECM structure or impeding wound closure. However, differences in fluorescent signal of the exogenous FN

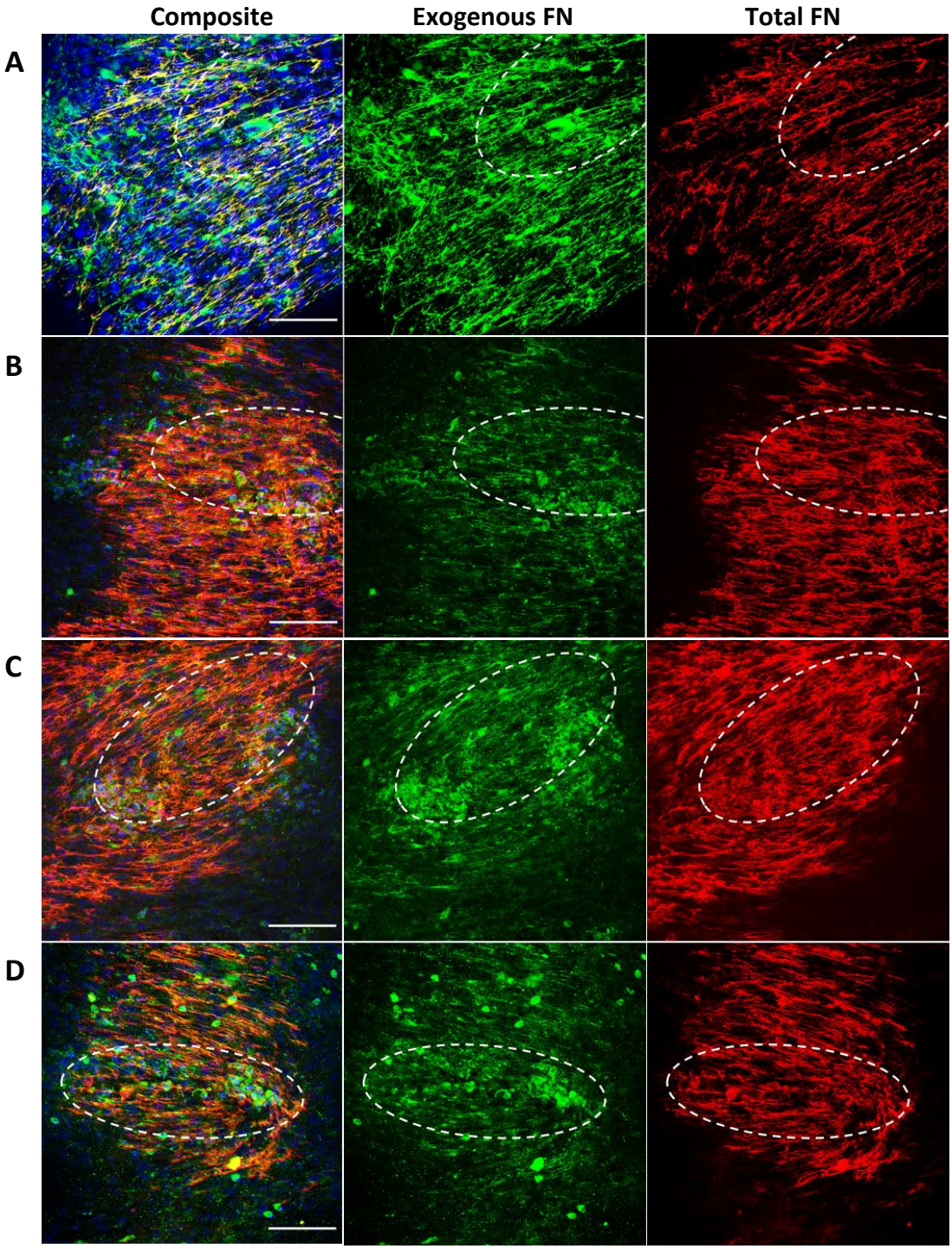

Figure 10: Microtissues with PEG-FN fragments (green) added during tissue formation, fixed after wounding and immunostained with anti-FN (red) and DAPI (blue), then imaged with confocal laser microscopy. (A) FN-AF488 50 nM (B) FN-PEG 50 nM (C) FN-PEG 150 nM (D) FN-PEG 250 nM. Estimated original wound sizes are marked with dashed lines. Composite images are in the first column. Scale bar: 100 μm.

indicate a lower recycling efficiency of PEGylated FN. FN recycling and the specific domains involved are areas of study that have not yet been explored; identifying nonessential domains within the fibronectin subunit can enhance our understanding of recycling and may facilitate enhanced recycling of synthetic conjugates.

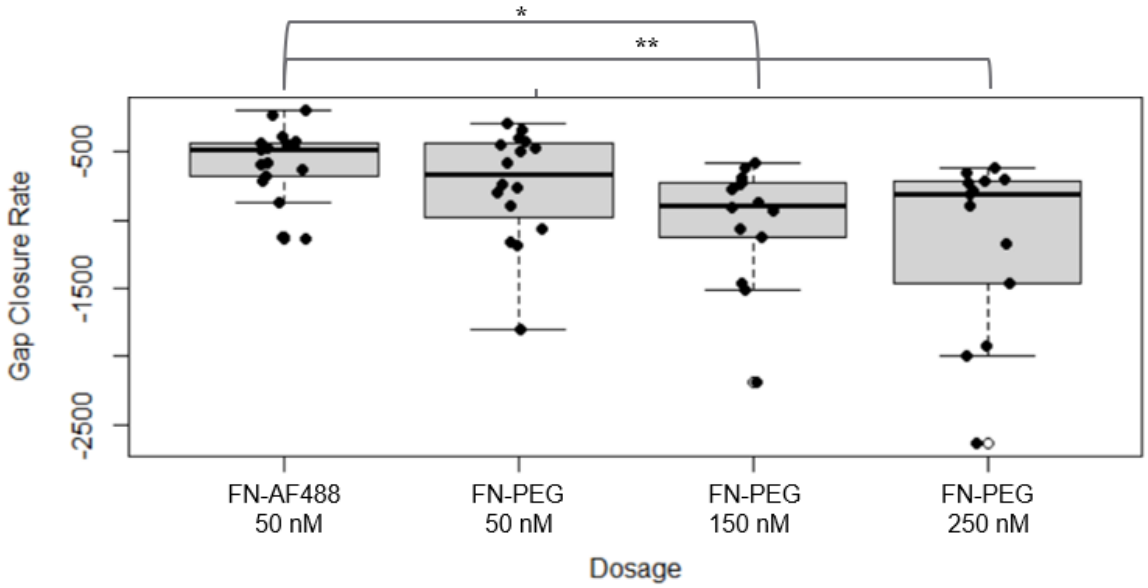

Figure 11: FN-AF488 (50 nM): -579.113 ± 265.4154 (n=17); FN-PEG (50 nM): -739.355 ± 405.9768 (n=16); FN-PEG (150 nM): -1011.67 ± 444.1084 (n=14); FN-PEG (250 nM): -1159.28 ± 647.0236 (n=13).

Aim 2: Explore functional domains of fibronectin and how they contribute to FN recycling

Single domains are not sufficient for recycling

As an initial screening to determine if FN fragments can be recycled and if single functional domains are sufficient for recycling, FN fragments generated by proteolytic cleavage (as portrayed in Figure 1) were labeled with AF dyes and added to microtissues. Confocal microscopy images found that the 30 kDa and 70 kDa fragments, which are involved in matrix assembly initiation, are able to assemble into short fibrils within the

provisional matrix, although they do not replicate the same fibrillar structure seen with full length FN-AF488 (Figure 12B-C). All other fragments produced by proteolytic cleavage are present within the provisional matrix but are unable to undergo the conformational changes for fibrillogenesis and appear to remain globular. EDA and EDB have low fluorescent signals and are likely to be endocytosed based on observations during imaging (Figure 12G-H). Based on total fibronectin staining, fragments may bind competitively and terminate fibrillogenesis, impacting structure of the native ECM. This confirms the results of previous studies conducted on 2D substrates, which found that binding of the 70 kDa fragment to fibroblasts blocks crosslinking and assembly of full-length fibronectin [31]. It should be noted that incomplete closure of the wound gap within 24h may not be solely due to addition of the fragments, but also to larger initial wound size of some microtissues. However, gap closure rates are impacted by FN domain availability. Microtissues with exogenously added full-length FN-AF488 healed at rates significantly different to those with 30 kDa and EDA (Figure 13). 30 kDa fragments correspond to the lowest slope of gap area closure, suggesting that this is the region within the 70 kDa fragment critical for the wound healing response and recycling. These results suggest that more than one domain may be necessary for recycling, leading to a fibronectin mimetic that interact with ECM molecules and cell surface receptors by joining multiple domains.

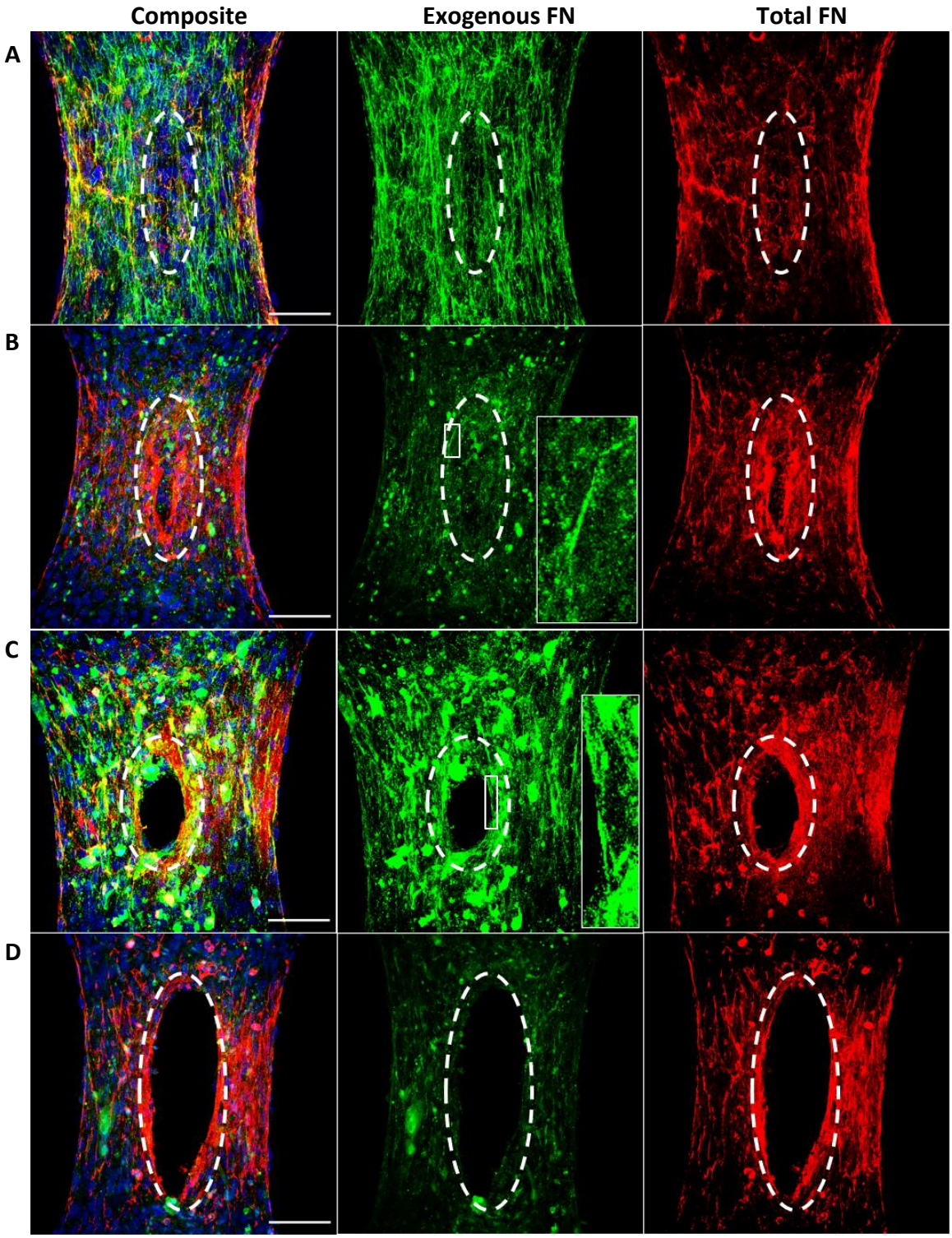
Composite
Exogenous FN
Total FN
A
B
C
D

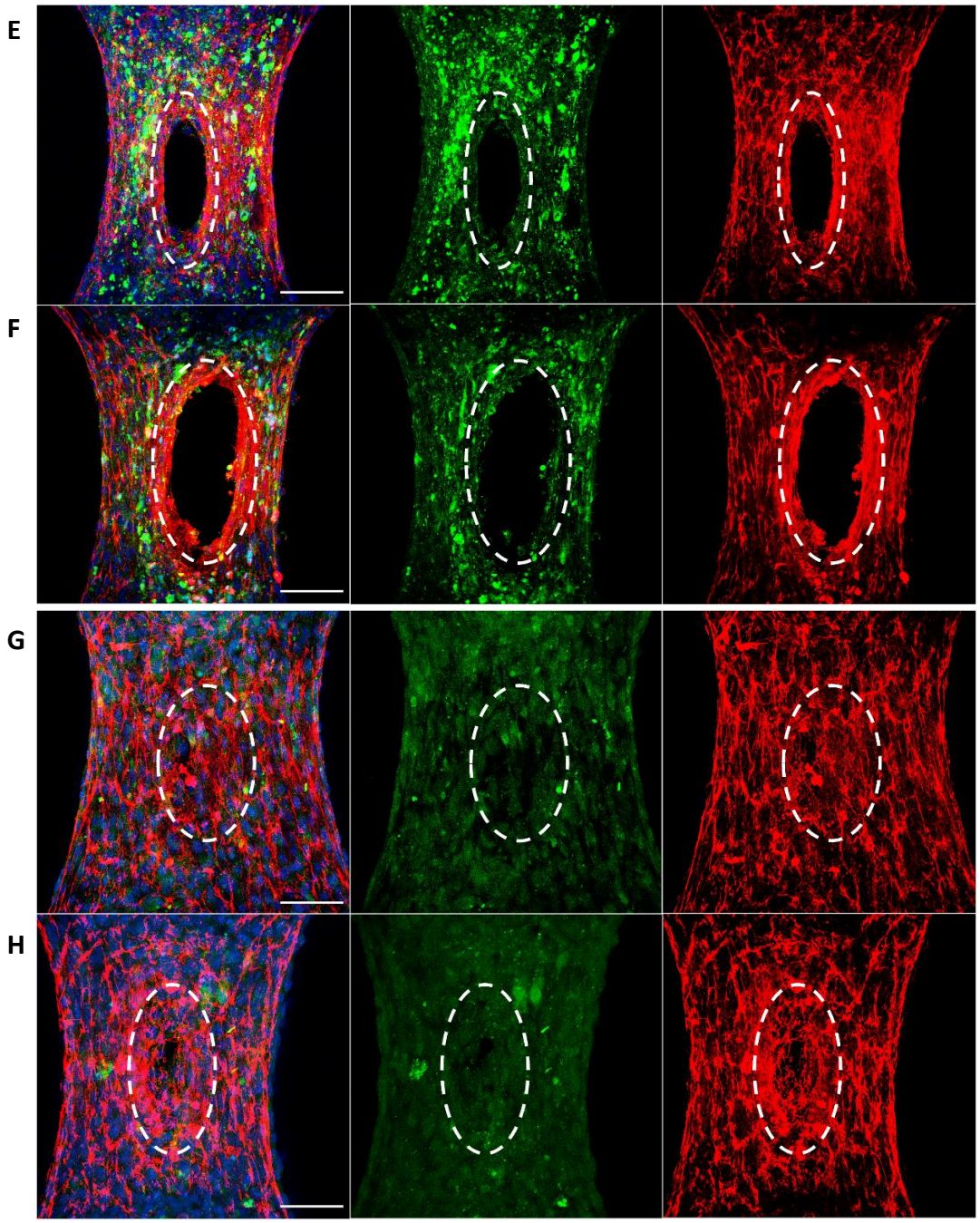

Figure 12: Microtissues with exogenous FN fragments (green) derived from proteolytic cleavage. Tissues fixed 24 hours after wounding and immunostained with anti-FN (red) and DAPI (blue), then imaged with confocal laser microscopy. (A) Full length FN-AF488 (B) 70 kDa (C) 30 kDa (D) 45 kDa (E) 40 kDa (F) 120 kDa (G) EDA (H) EDB. Estimated original wound sizes are marked with dashed lines. Insets show close ups of fibrils formed by exogenous fragments. Scale bar: 100 µm.

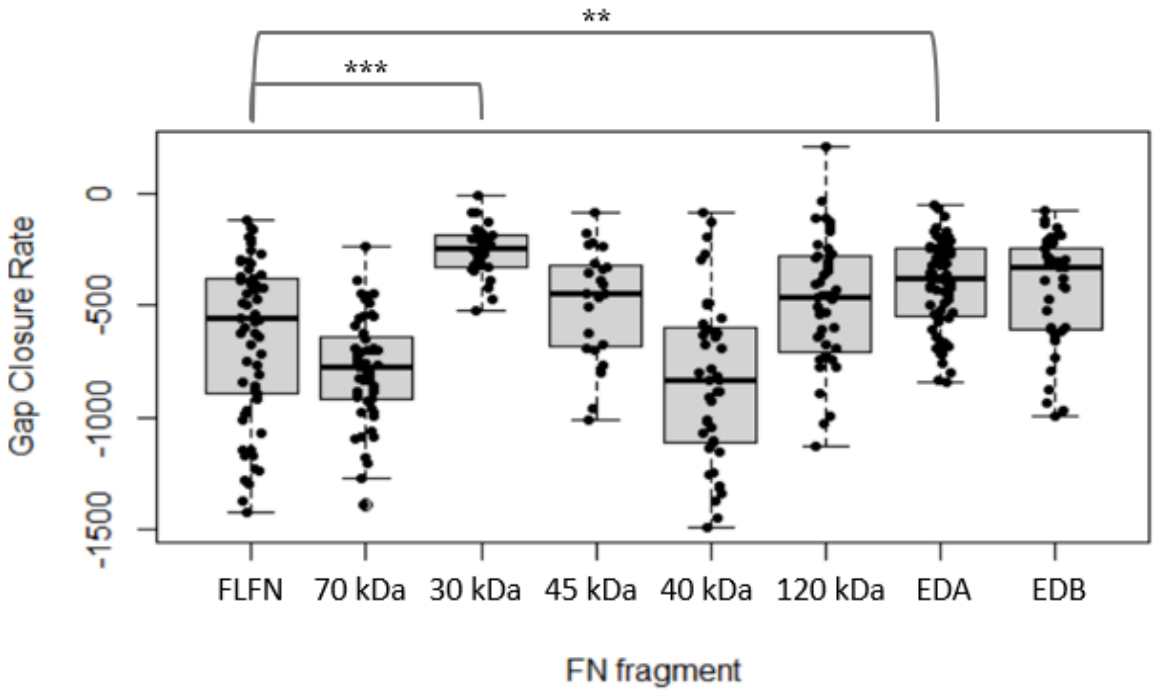

Figure 13: Effect of exogenous proteolytic FN fragments on microtissue wound healing and gap closure rates. Full length FN: -644.601 ± 352.8212 (n=62); 70 kDa: -783.1 ± 236.415 (n=52); 30 kDa: -258.43 ± 119.753 (n=26); 45 kDa: -484.062 ± 250.573 (n=23); 40 kDa: -830.135 ± 363.788 (n=43); 120 kDa: -486.921 ± 282.407 (n=44); EDA: -407.43 ± 196.234 (n=68); EDB: -430.608 ± 251.625 (n=38).

Chimeric FN mimetics are recycled and form fibrils

To determine if FN-based proteins with multiple functional domains would facilitate recycling, we looked towards chimeric FN mimetics that selectively joined bioactive regions that interact with both ECM proteins and cell surface receptors. Chimeric FN mimetics GST/III1H,8–10, GST/III1H,8^{RGD}, and GST/III1H^{RGD} were engineered as a substrate to stimulate cell growth, cell adhesion, and ECM production to a greater extent than full-length fibronectin. These mimetics connect a heparin binding site in type III repeat 1 (III1H) to a varying integrin binding domain that provides cell regulatory signals [21]. The molecular weights of the FN mimetics GST/III1H,8–10, GST/III1H,8^{RGD}, and GST/III1H^{RGD} are 65 kDa, 48 kDa, 37 kDa, respectively, which are much lower than that

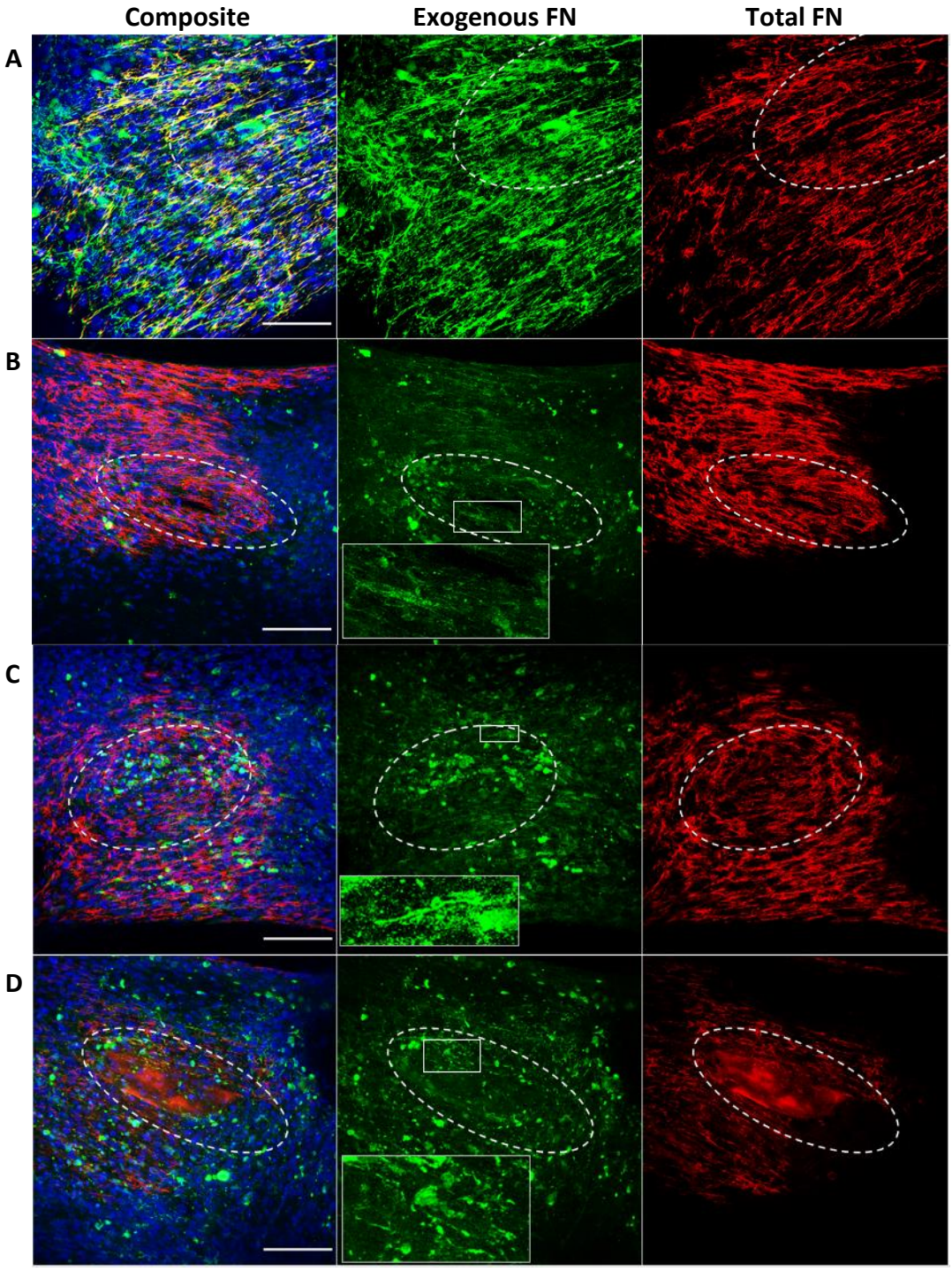

Figure 14: Microtissues with exogenous chimeric FN mimetics with heparin-binding domain and varying cell-binding domain. (A) FN-AF488 (B) GST/III1H,8–10 (C) GST/III1H,8^{RGD} (D) GST/III1H^{RGD}. Tissues fixed 24 hours after wounding and immunostained with anti-FN (red), anti-AF488 (green), and DAPI (blue), then imaged with confocal laser microscopy. Merged images in first column. Scale bar: 100 μm.

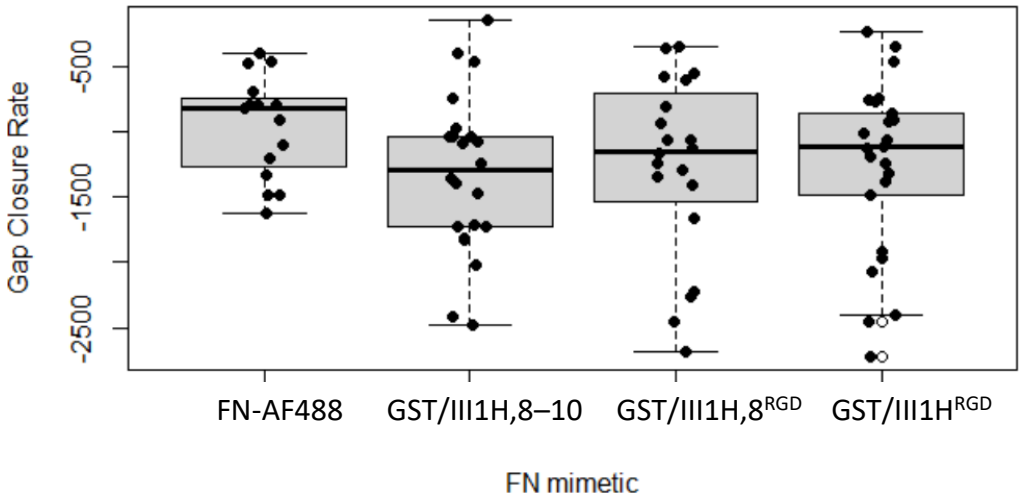

Figure 15: No significant difference in gap closure rates is found between microtissues with FN-AF488 and FN mimetics (50 nM). FN-AF488: -960.121 ± 394.441 (n=15); III1H,8-10: -1328.045 ± 609.7723 (n=22); III1H,8^{RGD}: -1260.292 ± 690.675 (n=20); $III1H^{RGD}$: -1261.428 ± 657.869 (n=25).

of a single full-length fibronectin subunit. Fibrils of all chimeric mimetics are observed within the provisional matrix of the wound gap (Figure 14), showing that they have been recruited by fibroblasts during wound healing and can be incorporated into a new matrix even without dimerization. Qualitatively, GST/III1H,8-10 is most successful at recycling and is able to assemble into longer fibrils, likely due to the binding site for repeat III_1 in repeat III_{10}. No significant difference is found between the gap closure rates of microtissues with full length fibronectin and chimeric mimetics (Figure 15).

Recombinant Fibronectin Design and Rationale

Informed by these results and by previous literature, recombinant proteins were designed with domains that have been identified as relevant to recycling to enhance recycling efficiency (Figure 8B). Derived from hpFN, each of the protein constructs (RecFN1-4) contain large deletions but no changes in structural order. The N-terminus fragment of constructs RecFN1 and RecFN2 consist of the 70 kDa domain (required for initiation and

assembly) and repeats III_{1-2}, which contain a cryptic binding site important for FN-FN crosslinking and fibril growth [23]. The N-terminus fragment is joined by a central cell-binding domain (III_{8-10}), which interacts with multiple integrins and contains another cryptic binding site. Construct RecFN1 contains the C-terminus disulfide bonds required for dimerization of FN subunits and subsequent fibrillogenesis, whereas RecFN2 does not. RecFN3 and RecFN4 are analogues to RecFN1 and RecFN2, respectively, that do not contain repeats III_{1-2}. All fragments were PCR amplified from a plasmid containing FN1 gene then inserted into a GST backbone, as described previously. A diagnostic restriction digest using XmaI and KpnI (Figure 16) confirms that correctly sized inserts are present for constructs RecFN1-4, and all plasmid sequences were confirmed with Sanger sequencing (data not shown).

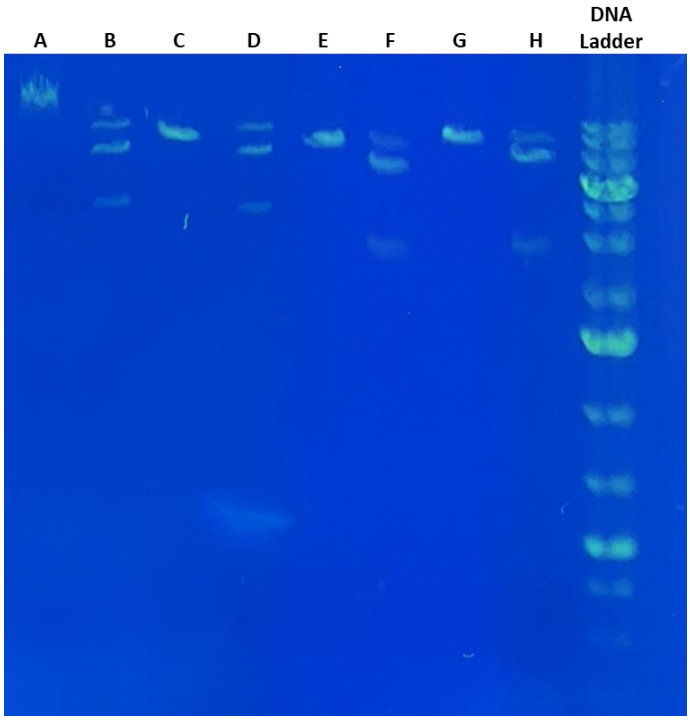

Figure 16: Gel electrophoresis results of plasmids containing RecFN1-4 constructs after double digest with labeled restriction enzymes. (A, C, E, G) Uncut GST-RecFN1-4 plasmids, respectively. (B, D, F, G) Double digested RecFN1-4 plasmids.

In addition to determining if RecFN proteins are more efficiently recycled than full length FN, studies with the recycling assay will confirm if dimerization if necessary for recycling and how presence of the cryptic binding sites in III_{1-2} contribute to matrix formation. Staining of microtissues formed with chimeric FN mimetics do not exhibit crosslinking of fibrils; it is hypothesized that inclusion of III_{1-2} will facilitate more complex fibrillar structure and interconnected networks as seen in control microtissues.

Aim 3: Assess biofunctionality of synthetic materials after integration into newly formed ECM

Biotin sites on biotinylated FN are still active and functional after undergoing recycling

To assess biofunctionality of FN conjugates after integration into native ECM, we introduced biotinylated FN to our recycling assay to see if biotin retains its function after it has been recycled. Streptavidin-AF488 is added to live tissues after complete healing and is positive throughout the provisional matrix (Figure 17). Given that streptavidin binds with high affinity to biotin and does not bind specifically to many other binding partners, this confirms that biotin sites are still available within the provisional matrix and builds on the results of the biotinylated FN recycling assay performed by Phillips, et al. on a 2D substrate [19]. Interestingly, streptavidin-AF488 signal was not restricted to the fibronectin fibers only but appeared as globular spots inside the repaired tissue area. Given that the signal co-localized with the DAPI signal in the nuclei of cells, we postulated that the streptavidin-488 detected intracellular biotin inside dead cells. Indeed, ethidium homodimer-1 staining for dead nuclei shows a similar pattern to dead cells at the edge of the repair tissue, which is in agreement with our hypothesis (Figure 18). No

significant difference was found between gap closure rates in microtissues with FN-AF488 and biotin-FN (Figure 19).

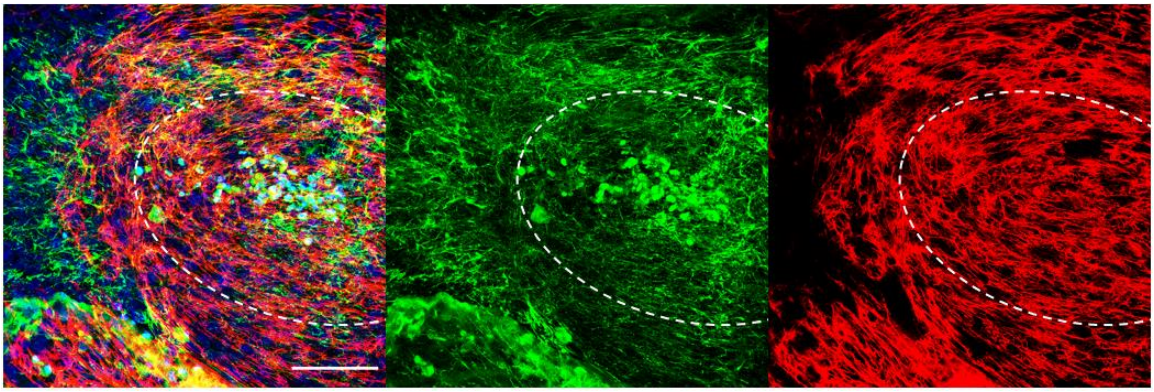

Figure 17: Microtissues with exogenous biotin-FN added before injury and streptavidin-AF488 added post complete wound healing. Tissues are immunostained with anti-FN (red) and DAPI (blue), then imaged with confocal laser microscopy. The merged image is shown on the left. Scale bar: 100 µm.

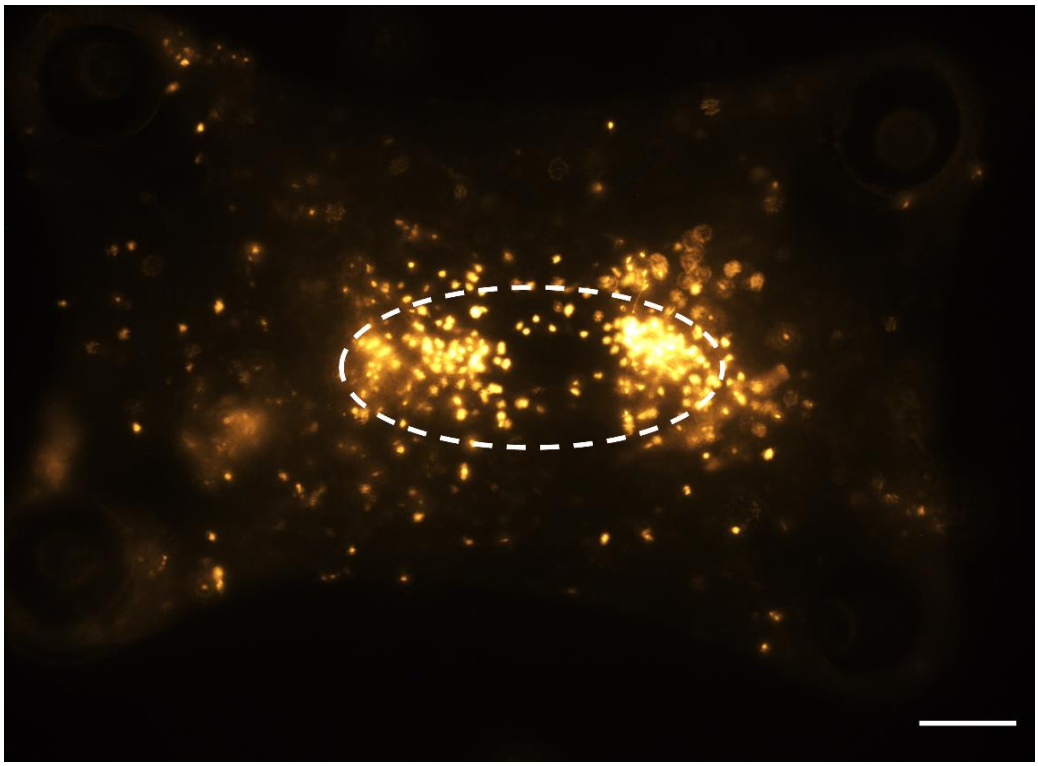

Figure 18: Ethidium homodimer-1 staining of cells in microtissue taken with Nikon Eclipse TE200. Dead cells are localized to corners of the ellipse formed by the wound boundary. Scale bar: 100 µm.

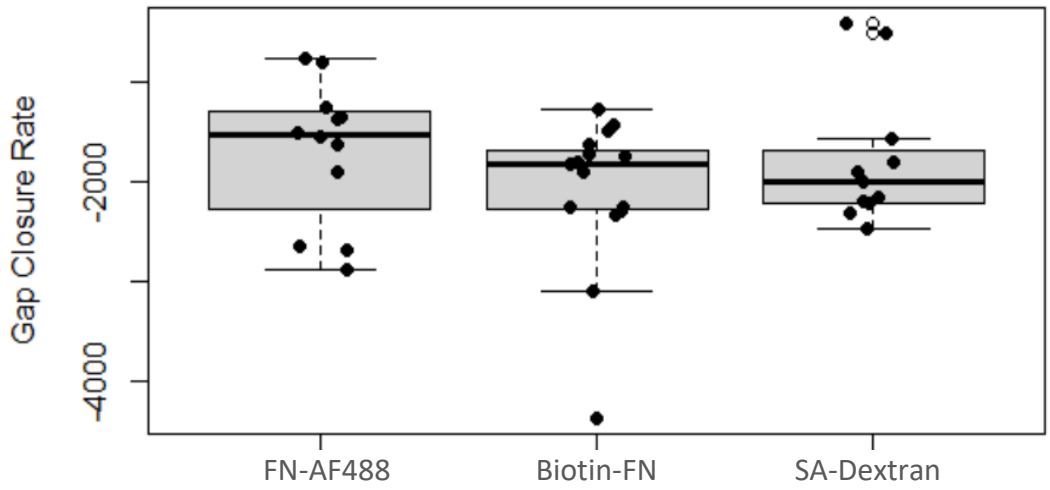

Figure 19: No significant difference in gap closure rates is found between microtissues with FN-AF488, biotin-FN and SA-dex, and biotin-FN only. FN-AF488: -1697.0468 ± 706.3315 (n=12); Biotin-FN: -2098.7627 ± 780.2304 (n=15); SA-dextran: -1779.4012 ± 699.9681 (n=11).

Given that structures developed by fragments and chimeric FN mimetics in microtissues are different from our control, we explored a different strategy to bring in materials that would not impact fibrillar structure. We introduced modified dextran with streptavidin conjugates (SA-dex) to the microtissues, with the hypothesis that adding in materials after a FN-biotin building block has been incorporated into the provisional matrix helps to retain their network structure. SA-dex was added in during tissue formation (TF) and post wound healing (PH) to determine how its addition would impact wound healing and fibrillar structure. While there was no significant difference found between the rates of gap closure between microtissues with TF-SA-dex and FN-AF488 (Figure 19), the addition of dextran during tissue formation did impact the structure of the biotin-FN matrix. SA-dex is not found in a fibrillar network and minimally colocalizes with the native FN matrix (insets in Figure 20A), likely having affected FN recycling and fibrillogenesis. However, PF-SA-dex microtissues exhibit high colocalization of dextran

with the native FN matrix, allowing dextran to mimic a fibrillar network structure.

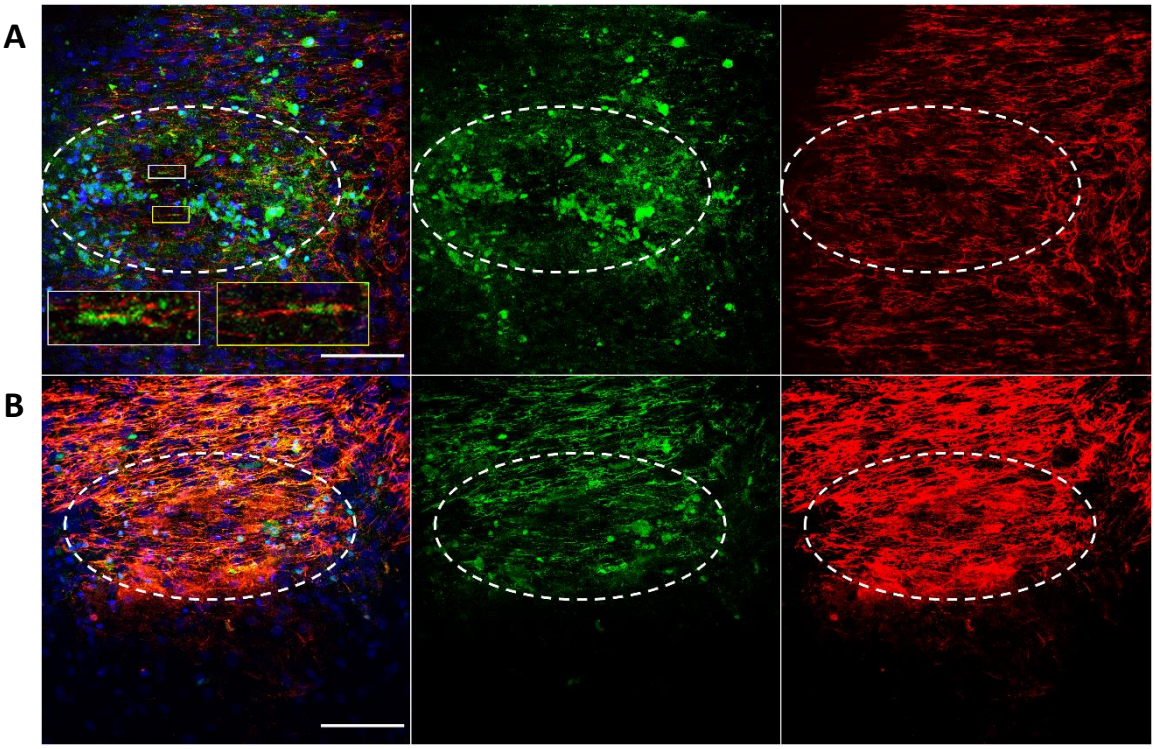

Figure 20: Microtissues with exogenous biotin-FN and SA-dex added to live tissue (A) during tissue formation or (B) SA-dex added post wound healing. Tissues are immunostained with anti-FN (red), anti-Dextran-FITC (green), and DAPI (blue), then imaged with confocal laser microscopy. Merged images are shown in the first column. Scale bar: 100 µm.

Comparison between controls

To confirm that there is no significant effect of labeling full-length FN with AF488 dyes, a wound assay was conducted to compare microtissues with unlabeled hpFN with FN-AF488. No significant difference is found in the gap closure rates between unlabeled FN and FN-AF488. The total FN matrix is also qualitatively similar to that of microtissues with FN-AF488 (Figure 21).

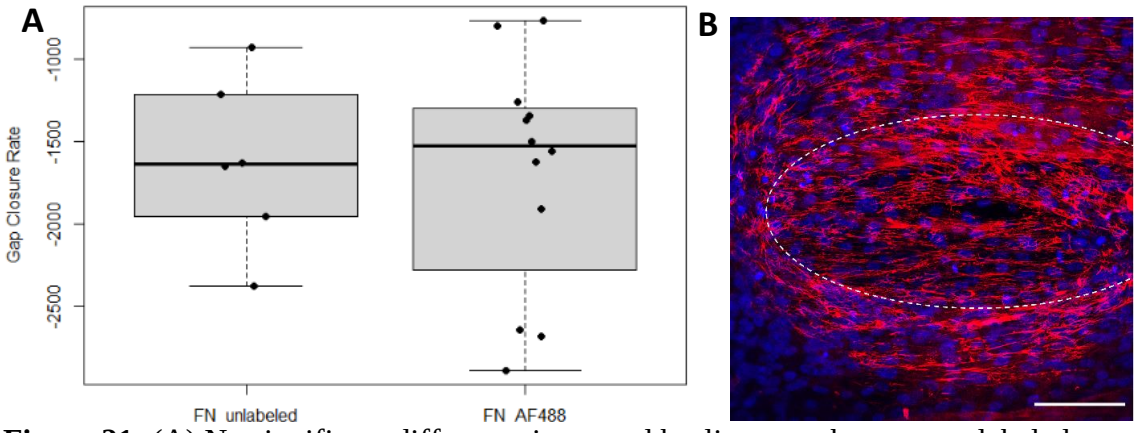

Figure 21: (A) No significant difference in wound healing rates between unlabeled human plasma fibronectin and fibronectin labeled with AF488 dyes. Unlabeled hpFN: -1626.97 ± 514.5377 (n=6); FN-AF488: -1697.0468 ± 706.3315 (n=12).
(B) Merged image of microtissue with unlabeled hpFN added during TF (50 nM). The tissue is fixed and immunostained with anti-FN (red) and DAPI (blue), then imaged with confocal laser microscopy. Scale bar: 100 µm.

7. DISCUSSION

In this thesis, we explored the concept of fibronectin recycling by generating fibronectin-based materials and delivering them to a biomimetic wound healing model to assess their recycling during an *in vitro* wound healing response. The results show that when conjugated with FN, synthetic materials such as PEG can undergo recycling and fibrillogenesis in microtissues with no significant changes in wound healing rates. This expands upon previous work which found that FN-PEG can be assembled by cells into fibrils when immobilized on surfaces [34]. They determined that PEGylating FN with a higher molecular weight PEG had a direct relationship with improving proteolytic stability and detected no significant changes to the secondary structure of FN after PEGylation with 2, 5, and 10 kDa mPEG-SCM molecules. However, PEGylation presents steric hindrances that led to a decrease in cell adhesion, cell spreading, and gelatin binding, indicating that functional domains within FN are less accessible. This may reduce cells' ability to recycle FN-PEG and assemble them into fibrils, which is observed in Figure 10. In immunoblotting experiments, antibodies against PEG were not able to detect FN-PEG, likely due to the low affinity of anti-PEG antibodies to the antigen. Though a positive result using anti-FITC antibodies confirms that the FN is PEGylated, the average number of PEG molecules per FN could not be parsed out via immunoblotting techniques.

Hocking and Kowalski found that cell interaction with recombinant FN constructed by joining heparin binding fragment III1H to integrin binding modules stimulates cell growth and contractility, while either domain alone was ineffective [10]. While these FN

mimetics were designed to coat surfaces on which cells are seeded, we assessed them in a 3D substrate in which they were dynamically remodeled into the tissue. This presents additional constraints in how cells recognize and process the proteins, possibly treating them as a foreign material. Even so, the chimeric mimetics were all able to assemble into short fibrils within the provisional matrix of the original wound area, suggesting that interactions with both ECM proteins and cells contribute to a recycling capability in recombinant FN, and that dimerization may not be necessary for recycling despite being a requirement for fibrillogenesis and matrix assembly.

No fibrillogenesis is seen with TF-SA-dex, confirming that adding synthetic materials to nonspecific sites via NHS labeling can impact recycling. Site-specific labeling can be achieved by incorporating SNAP tags or unnatural amino acids [13] to less functionally important areas of the protein. While fragments and chimeric mimetics were not able to form fibrillar matrices on their own, the approach of adding dextran to a tissue with integrated biotin-FN post healing utilizes an existing FN matrix to build a dextran matrix that mimics its crosslinked structure. Modifying dextran to sequester growth factors or drug conjugates and tethering them to the ECM could provide a new approach to drug delivery, regulate cell processes such as proliferation and adhesion, or alter mechanical properties of the ECM.

Metalloproteinases play an important role in fibronectin endocytosis, intracellular degradation, or recycling back to the cell surface. As mature FN fibrils are insoluble, metalloproteinases are necessary for cleaving extracellular FN and this process is mediated by integrins [19]. The connection between endocytosis and fibronectin

degradation is not completely clear; internalized FN may get recycled or degraded depending on factors that require more insight. An early study by Sottile and Chandler focusing on the degradation pathway showed that FN turnover occurs through a caveolin-1 dependent process [26], whereas overexpression of deubiquitinase USP10 leads to increased recycling by preventing degradation of integrins α5ß1 and αv [19]. Future mechanistic studies using recombinant proteins and chimeric fibronectin fragments can provide further insights on the recycling pathway.

8. CONCLUSION AND FUTURE PERSPECTIVES

By exploiting the recycling mechanism of FN, we demonstrate that synthetically modified FN can be used as a building block to integrate synthetic materials into newly formed ECM during wound healing. Studies with proteolytically cleaved fragments and chimeric FN mimetics suggest that more than one functional domain within FN is necessary for recycling, and that interactions with ECM proteins and cells are required for reincorporation of recycled material into fibrils. Insights into the domains relevant for recycling led to the design of recombinant FN proteins that may exhibit enhanced recycling ability. Importantly, we show that FN-PEG and biotinylated FN can undergo recycling and are integrated into nascent tissue, and that recycled biotin-FN retains its bioactive sites for binding partners.

New therapies based on recyclable synthetic biomaterials can be designed to retain synthetic control of biological activity, the basis of which has been demonstrated by this work. By moving past the approach of biomaterials that interface with cells to integrating new materials that will dynamically remodel with cells into nascent tissue, these materials can serve as targets for drug delivery and inspire new approaches to engineering tissues *in vitro* or *in situ*.

BIBLIOGRAPHY

1. Almany, L. and D. Seliktar, *Biosynthetic hydrogel scaffolds made from fibrinogen and polyethylene glycol for 3D cell cultures.* Biomaterials, 2005. **26**(15): p. 2467–2477.

2. Ammassam Veettil, R., et al., *Dextran Sulfate Polymer Wafer Promotes Corneal Wound Healing.* Pharmaceutics, 2021. **13**(10): p 1628. https://doi.org/10.3390/pharmaceutics13101628

3. Barry, E.L. and D.F. Mosher, *Factor XIII cross-linking of fibronectin at cellular matrix assembly sites.* Journal of Biological Chemistry, 1988. **263**(21): p. 10464–10469.

4. Bridgewater, R.E., J.C. Norman, and P.T. Caswell, *Integrin trafficking at a glance.* Journal of Cell Science, 2012. **125**(Pt 16): p. 3695–3701.

5. Cengiz-Çallıoğlu, F., *Dextran nanofiber production by needleless electrospinning process.* e-Polymers, 2014. **14**(1): p. 5–13. https://doi.org/10.1515/epoly-2013-0021

6. Dalton, C.J. and C.A. Lemmon, *Fibronectin: Molecular Structure, Fibrillar Structure and Mechanochemical Signaling.* Cells, 2021. **10**(9): p. 2443. https://dx.doi.org/10.3390%2Fcells10092443

7. Gee, E.P.S., et al., *SLLISWD Sequence in the 10FNIII Domain Initiates Fibronectin Fibrillogenesis.* Journal of Biological Chemistry, 2013. **288**(29): p. 21329–21340.

8. Grant, B.D. and J.G. Donaldson, *Pathways and mechanisms of endocytic recycling.* Nature Reviews. Molecular Cell Biology, 2009. **10**(9): p. 597–608.

9. Hiraguchi, Y., et al., *Effect of the distribution of adsorbed proteins on cellular adhesion behaviors using surfaces of nanoscale phase-reversed amphiphilic block copolymers.* Acta Biomaterialia, 2014. **10**(7): p. 2988–2995.

10. Hocking, D.C. and K. Kowalski, *A cryptic fragment from fibronectin's III1 module localizes to lipid rafts and stimulates cell growth and contractility.* Journal of Cell Biology, 2002. **158**(1): p. 175–184.

11. Hocking, D.C., J. Sottile, and P.J. McKeown-Longo, *Fibronectin's III-1 module contains a conformation-dependent binding site for the amino-terminal region of fibronectin.* Journal of Biological Chemistry, 1994. **269**(29): p. 19183-19187.

12. Langer, R. and J.P. Vacanti, *Tissue engineering.* Science, 1993. **260**(5110): p. 920-926.

13. Lee, K.J., D. Kang, and H.S. Park, *Site-Specific Labeling of Proteins Using Unnatural Amino Acids.* Molecules and Cells, 2019. **42**(5): p. 386–396. https://doi.org/10.14348/molcells.2019.0078

14. Mao, Y. and J.E. Schwarzbauer, *Fibronectin fibrillogenesis, a cell-mediated matrix assembly process.* Matrix Biology, 2005. **24**(6): p. 389–399.

15. Martino, M.M., et al., *Heparin-binding domain of fibrin(ogen) binds growth factors and promotes tissue repair when incorporated within a synthetic matrix.* 2013. Proceedings of the National Academy of Sciences of the United States of America, **110**(12): p. 4563–4568. https://doi.org/10.1073/pnas.1221602110

16. Ouyang, L., et al., *MMP-sensitive PEG hydrogel modified with RGD promotes bFGF, VEGF and EPC-mediated angiogenesis.* Experimental and Therapeutic Medicine, 2019. **18**(4): p. 2933–2941.

17. Pankov, R. and K.M. Yamada, *Fibronectin at a glance.* Journal of Cell Science, 2002. **115**(20): p. 3861–3863.

18. Parisi, L., et al., *A glance on the role of fibronectin in controlling cell response at biomaterial interface.* Japanese Dental Science Review, 2020. **56**(1): p. 50–55.

19. Phillips, A.T., et al., *USP10 Promotes Fibronectin Recycling, Secretion, and Organization.* Investigative Ophthalmology & Visual Science, 2021. **62**(13): p. 15.

20. Revzin, A., et al., *Fabrication of Poly(ethylene glycol) Hydrogel Microstructures Using Photolithography.* Langmuir, 2001. **17**(18): p. 5440–5447.

21. Roy, D.C., S.J. Wilke-Mounts, and D.C. Hocking, *Chimeric fibronectin matrix mimetic as a functional growth- and migration-promoting adhesive substrate.* Biomaterials, 2011. **32**(8): p. 2077–2087.

22. Sakar, M.S., et al., *Cellular forces and matrix assembly coordinate fibrous tissue repair.* Nature Communications, 2016. **7**(1): p. 11036.

23. Sechler, J.L., et al., *A novel fibronectin binding site required for fibronectin fibril growth during matrix assembly.* Journal of Cell Biology, 2001. **154**(5): p. 1081–1088.

24. Sechler, J.L., Y. Takada, and J.E. Schwarzbauer, *Altered rate of fibronectin matrix assembly by deletion of the first type III repeats.* Journal of Cell Biology, 1996. **134**(2): p. 573–583.

25. Shaterabadi, Z., G. Nabiyouni, and M. Soleymani, *High impact of in situ dextran coating on biocompatibility, stability and magnetic properties of iron oxide nanoparticles.* Materials Science & Engineering. C, Materials for Biological Applications, 2017. **75**: p. 947–956.

26. Shi, F. and J. Sottile, *Caveolin-1-dependent beta1 integrin endocytosis is a critical regulator of fibronectin turnover.* Journal of Cell Science, 2008. **121**(Pt 14): p. 2360–2371.

27. Sun, G. and C.-C. Chu, *Self-Assembly of Chemically Engineered Hydrophilic Dextran into Microscopic Tubules.* ACS Nano, 2009. **3**(5): p. 1176–1182.

28. Sun, G. and J.J. Mao, *Engineering dextran-based scaffolds for drug delivery and tissue repair.* Nanomedicine (London, England), 2012. **7**(11): p. 1771–1784.

29. Takahashi, S., et al., *The RGD motif in fibronectin is essential for development but dispensable for fibril assembly.* Journal of Cell Biology, 2007. **178**(1): p. 167–718.

30. To, W.S. and K.S. Midwood, *Plasma and cellular fibronectin: distinct and independent functions during tissue repair.* Fibrogenesis & Tissue Repair, 2011. **4**: p. 21.

31. Tomasini-Johansson, B.R., D.S. Annis, and D.F. Mosher, *The N-terminal 70-kDa fragment of fibronectin binds to cell surface fibronectin assembly sites in the absence of intact fibronectin.* Matrix Biology, 2006. **25**(5): p. 282–293.

32. Varadaraj, A., et al., *TGF-β triggers rapid fibrillogenesis via a novel TβRII-dependent fibronectin-trafficking mechanism.* Molecular Biology of the Cell, 2017. **28**(9): p. 1195–1207.

33. White, E.S., F.E. Baralle, and A.F. Muro, *New insights into form and function of fibronectin splice variants.* Journal of Pathology, 2008. **216**(1): p. 1–14.

34. Zhang, C., et al., *PEGylation of lysine residues improves the proteolytic stability of fibronectin while retaining biological activity.* Biotechnology Journal, 2014. **9**(8): p. 1033–1043.

35. Zhu, J., *Bioactive modification of poly(ethylene glycol) hydrogels for tissue engineering.* Biomaterials, 2010. **31**(17): p. 4639–4656.

CURRICULUM VITAE